

# Fe–H Complexes in Catalysis

Hiroshi Nakazawa and Masumi Itazaki

**Abstract** Organic syntheses catalyzed by iron complexes have attracted considerable attention because iron is an abundant, inexpensive, and environmentally benign metal. It has been documented that various iron hydride complexes play important roles in catalytic cycles such as hydrogenation, hydrosilylation, hydroboration, hydrogen generation, and element–element bond formation. This chapter summarizes the recent developments, mainly from 2000 to 2009, of iron catalysts involving hydride ligand(s) and the role of Fe–H species in catalytic cycles.

**Keywords** Catalysis · Electrochemical reduction · Hydroboration · Hydrogenation · Hydrosilylation · Iron hydride complex · Photochemical reduction

## Contents

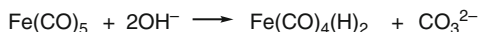
1	Introduction .....	28
2	Hydrogenation .....	30
2.1	Alkene and Alkyne Reduction .....	30
2.2	Ketone and Aldehyde Reduction .....	35
3	Hydrometalation .....	44
3.1	Hydrosilylation .....	44
3.2	Hydroboration .....	50
4	Organic Synthesis .....	52
4.1	C–C and C–E Bond Formation .....	52
4.2	Others .....	59
5	Hydrogen Generation .....	65
5.1	Electrochemical Reduction .....	66
5.2	Photochemical Reduction .....	72
	Appendix .....	74
	References .....	76

# 1 Introduction

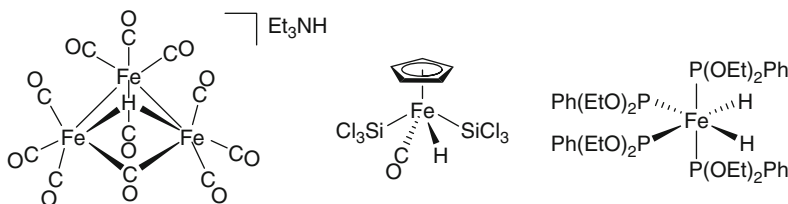
This chapter treats iron complexes with Fe–H bond(s). An H ligand on a transition metal is named in two ways, “hydride” and “hydrido.” The term “hydrido” is recommended to be used for hydrogen coordinating to all elements by IUPAC recommendations 2005 [1]. However, in this chapter, the term “hydride” is used because it has been widely accepted and used in many scientific reports.

In 1931, Hieber and Leutert reported  $\text{Fe}(\text{CO})_4(\text{H})_2$  not only as the first iron hydride complex but also as the first transition-metal hydride complex ( $\text{FeH}_2$  was reported in 1929 from  $\text{FeCl}_2$  and  $\text{PhMgBr}$  under a hydrogen atmosphere. However, it exists only in a gas phase) [2, 3]. The complex synthesized from  $\text{Fe}(\text{CO})_5$  and  $\text{OH}^-$  (Scheme 1) is isolable only at low temperature and decomposes at room temperature into  $\text{Fe}(\text{CO})_5$ ,  $\text{Fe}(\text{CO})_3$ , and  $\text{H}_2$ .

**Scheme 1** The first iron hydride complex

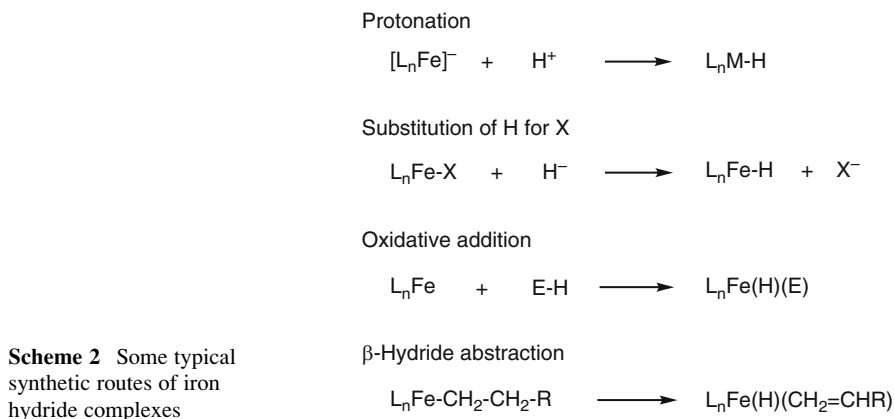


Since then, many iron hydride complexes have been prepared, isolated, characterized spectroscopically and, in some cases, by X-ray analyses. Hydrides show diagnostic signals in  $^1\text{H}$  NMR spectra. They resonate to high field in a region (0 ~ –60 ppm) for diamagnetic iron hydride complexes. Paramagnetic hydride complexes, however, are very difficult to characterize. IR spectra are helpful because Fe–H stretching frequencies are observed in the range of 1,500–2,200  $\text{cm}^{-1}$ . However, it should be noted that the intensities are often weak and hence the method is not entirely reliable. Crystallographic methods are generally powerful to obtain 3D arrangements and metrical data. However, hydrides, in some cases, are not detected because the hydride in the neighborhood of the metal is such a poor scatterer of X-rays. In addition, Fe–H bond distances should be carefully used because X-ray methods often underestimate the true Fe–H internuclear distance by approximately 0.1 Å. The X-ray structure of  $[\text{NEt}_3\text{H}][\text{HFe}_3(\text{CO})_{11}]$  having  $\mu\text{-H}$  ligand was reported in 1965 [4]. This compound might be the first structurally characterized iron complex bearing an H ligand (Fig. 1). The first terminal hydride iron complex characterized by the X-ray analysis was  $\text{CpFeH}(\text{CO})(\text{SiCl}_3)_2$ , in 1970 [5]. In 1972, the X-ray structure of *cis*- $[\text{Fe}(\text{H})_2\{\text{PPh}(\text{OEt})_2\}_4]$  was reported as the first dihydride iron complex [6] (Fig. 1).



**Fig. 1** The first X-ray crystal structures of three types of the iron hydride complexes

Iron hydride complexes can be synthesized by many routes. Some typical methods are listed in Scheme 2. Protonation of an anionic iron complex or substitution of hydride for one electron donor ligands, such as halides, affords hydride complexes.  $\text{NaBH}_4$  and  $\text{LiAlH}_4$  are generally used as the hydride source for the latter transformation. Oxidative addition of  $\text{H}_2$  and  $\text{E-H}$  to a low valent and unsaturated iron complex gives a hydride complex. Furthermore,  $\beta$ -hydride abstraction from an alkyl iron complex affords a hydride complex with olefin coordination. The last two reactions are frequently involved in catalytic cycles.



A Fe-H bond is generally polarized as  $\text{Fe}^{\delta+}\text{-H}^{\delta-}$  because H is more electronegative than Fe. However, iron hydride complexes impart much less negative charge to the hydride than early transition-metal hydride complexes.

Organic syntheses catalyzed by complexes of precious metals (Pd, Pt, Rh, Ir, Ru, etc.) have attracted considerable attention because both catalytic activities and chemo- and region selectivities are superior to those of heterogeneous catalysts. In order to understand the underlying principles of homogeneous catalysis, the reaction mechanisms are under intense investigation. For a large number of mechanisms, it has been well-established that various hydride complexes act as important intermediates in the catalytic cycle for hydrometalations such as, e.g., hydrosilylations or in hydrogenation reactions [7]. Furthermore, iron hydride complexes were shown to play pivotal roles in fundamental organometallic chemistry [8–11].

Precious metals have faced a significant price increase and the fear of depletion. By contrast, iron is a highly abundant metal in the crust of the earth (4.7 wt%) of low toxicity and price. Thus, it can be defined as an environmentally friendly material. Therefore, iron complexes have been studied intensively as an alternative for precious-metal catalysts within recent years (for reviews of iron-catalyzed organic reactions, see [12–20]). The chemistry of iron complexes continues to expand rapidly because these catalysts play indispensable roles in today's academic study as well as chemical industry.

This chapter summarizes the development of iron catalysts involving hydride ligand(s) and the role of the Fe–H species in the catalytic cycle in the past decade (2000–2009).

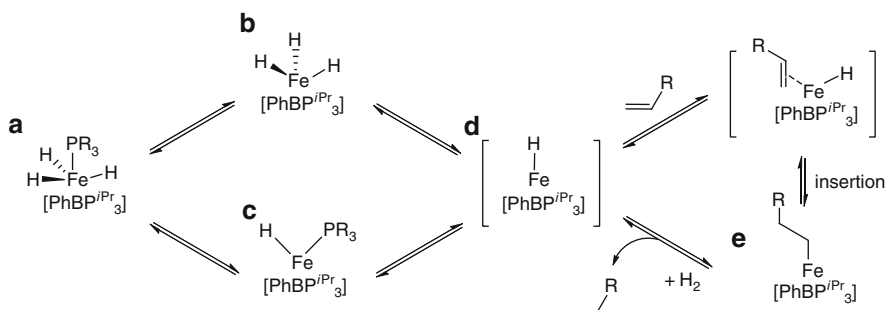
## 2 Hydrogenation

Reduction of unsaturated organic substrates such as alkenes, alkynes, ketones, and aldehydes by molecular dihydrogen or other H-sources is an important process in chemistry. In hydrogenation processes some iron complexes have been demonstrated to possess catalytic activity. Although catalytic intermediates have rarely been defined, the Fe–H bond has been thought to be involved in key intermediates.

### 2.1 Alkene and Alkyne Reduction

Until recently, iron-catalyzed hydrogenation reactions of alkenes and alkynes required high pressure of hydrogen (250–300 atm) and high temperature (around 200°C) [21–23], which were unacceptable for industrial processes [24, 25]. In addition, these reactions showed low or no chemoselectivity presumably due to the harsh reaction conditions. Therefore, modifications of the iron catalysts were desired.

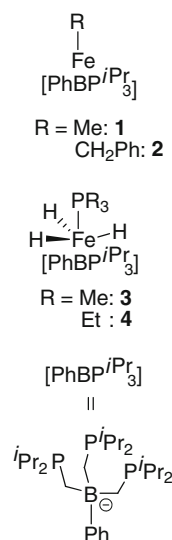
In 2004, Peters and Daida reported the hydrogenation of olefins catalyzed by iron complexes **1–4** having the tris(diisopropylphosphino)borate ligand,  $[\text{PhBP}^{\text{iPr}}_3]^-$ , under mild conditions (low pressure and ambient temperature) (Table 1) [26]. Although these catalytic activities were not high, a plausible reaction mechanism has been proposed (Scheme 3). The iron(IV) trihydride phosphine complex **a** being spectroscopically well-defined undergoes hydrogen loss to give the coordinatively unsaturated mono hydride complex **d**. Two pathways from **a** to **d** are conceivable: (1) the trihydride complex **b**, which is a detectable species by NMR, and (2) the monohydride phosphine complex **c**, which can be structurally identified when  $\text{PR}_3 = \text{PMePh}_2$ . Olefin coordination to **d** and its insertion into the Fe–H bond affords the stable alkyl complex **e**. This iron alkyl complex reacts with hydrogen to release the alkane with regeneration of the active species **d**.



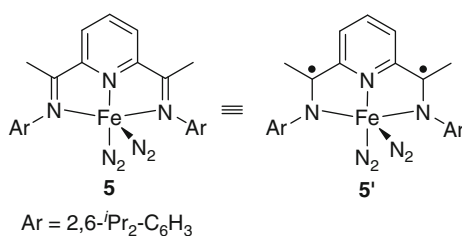
**Scheme 3** Plausible pathway for hydrogenation of olefin catalyzed by the Fe–H complex

**Table 1** Olefin hydrogenation reactions catalyzed by iron complexes

$\text{CH}_2=\text{CH-R} \xrightarrow[\text{H}_2, 23^\circ\text{C}]{10 \text{ mol\% cat.}} \text{CH}_3\text{CH}_2\text{-R}$				
Catalyst	Substrate	H <sub>2</sub> (atm)	Time (min)	TOF (mol/h)
1	Styrene	4	78	7.7
2	Styrene	4	100	6.0
2	Styrene	1	410	1.5
2	Ethylene	4	25	24.0
2	1-Hexene	1	130	4.6
1	1-Hexene	1	115	5.2
2	Cyclooctene	1	55	10.9
2	2-Pentyne	1	370	1.6
3 <sup>a</sup>	Styrene	1	1260	0.5
4	Styrene	1	1010	0.6

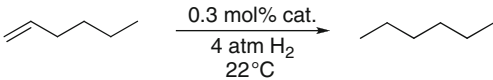
<sup>a</sup>Hydrogenation carried out at 50°C.

Bis(imino)pyridine iron complex **5** as a highly efficient catalyst for a hydrogenation reaction was synthesized by Chirik and coworkers in 2004 [27]. Complex **5** looks like a Fe(0) complex, but detailed investigations into the electronic structure of **5** by metrical data, Mössbauer parameters, infrared and NMR spectroscopy, and DFT calculations established the Fe(II) complex described as **5'** in Fig. 2 to be the higher populated species [28].

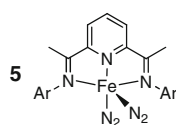
**Fig. 2** Bis(imino)pyridine iron complex

Complex **5** was more active than the well-known precious-metal catalysts (palladium on activated carbon Pd/C, the Wilkinson catalyst RhCl(PPh<sub>3</sub>)<sub>3</sub>, and Crabtree's catalyst [Ir(cod)(PCy<sub>3</sub>)py]PF<sub>6</sub>) and the analogous *N*-coordinated Fe complexes **6–8** [29] for the hydrogenation of 1-hexene (Table 2). In mechanistic studies, the NMR data revealed that **5** was converted into the dihydrogen complex **9** via the monodinitrogen complex under hydrogen atmosphere (Scheme 4).

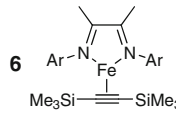
**Table 2** Comparison of iron complexes with transition precious-metal catalysts for the hydrogenation of 1-hexene

			
Catalyst	Time (min)	TOF (mol/h)	Ref.
<b>5</b>	12	1814	[27]
10% Pd/C	12	366	[27]
RhCl(PPh <sub>3</sub> ) <sub>3</sub>	12	10	[27]
[Ir(cod)(PCy <sub>3</sub> )py]PF <sub>6</sub>	12	75	[27]
<b>6</b> <sup>a</sup>	1440	4	[29]
<b>7</b>	240	90	[29]
<b>8</b>	240	90	[29]

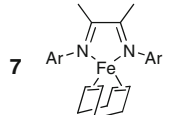
**5**



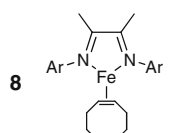
**6**



**7**



**8**



Ar = 2,6-*i*-Pr<sub>2</sub>-C<sub>6</sub>H<sub>3</sub>

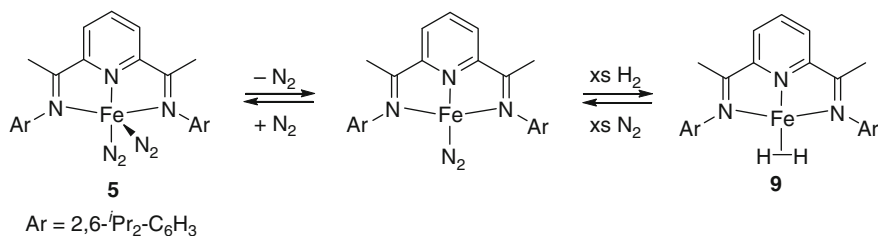
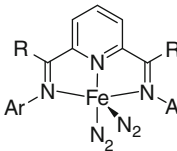
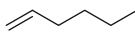
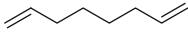
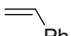
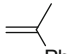

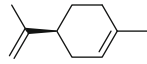
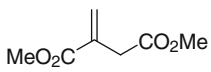
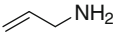
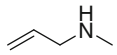
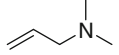
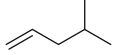
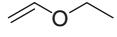
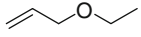
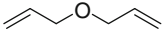
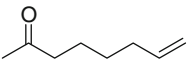
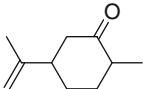
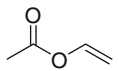
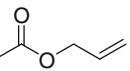
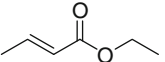
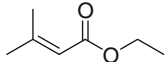
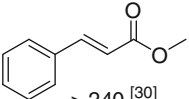
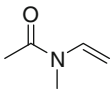
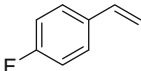
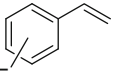
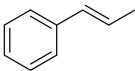
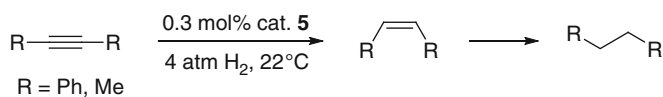
<sup>a</sup>Hydrogenation carried out at 60°C.**Scheme 4** Reaction of **5** under hydrogen atmosphere

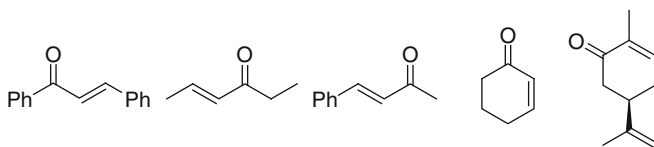
Table 3 summarizes the scope and limitation of substrates for this hydrogenation. Complex **5** acts as a highly effective catalyst for functionalized olefins with unprotected amines (the order of activity: tertiary > secondary ≫ primary), ethers, esters, fluorinated aryl groups, and others [27, 30]. However, in contrast to the reduction of  $\alpha,\beta$ -unsaturated esters decomposition of **5** was observed when  $\alpha,\beta$ -unsaturated ketones (e.g., *trans*-chalcone, *trans*-4-hexen-3-one, *trans*-4-phenyl-3-buten-2-one, 2-cyclohexanone, carvone) were used (Fig. 3) [30].

With internal alkynes such as diphenylacetylene and 2-butyne, the perhydrogenated products were formed in the presence of complex **5** via the corresponding *cis*-2-alkene as an intermediate (Scheme 5). In case of terminal alkynes such as trimethylsilylacetylene, the desired product was not formed.

**Table 3** Catalytic hydrogenation of various olefins with **5**

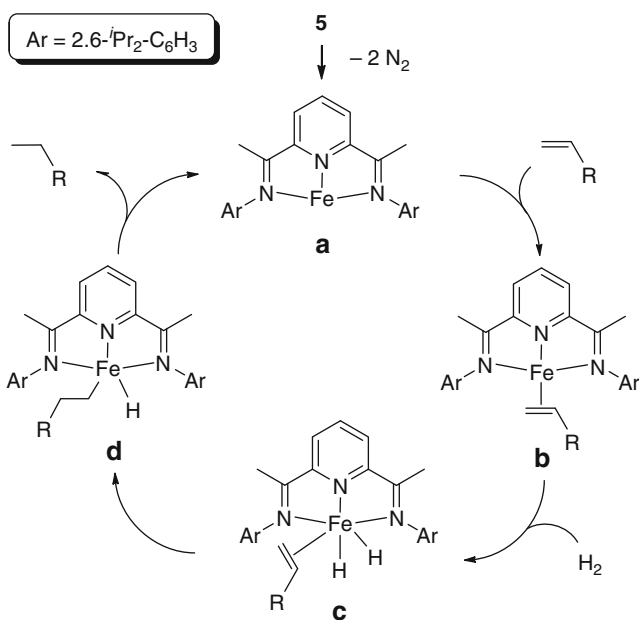
$\text{CH}_2=\text{CH-R} \xrightarrow[\text{toluene or neat, 23}^\circ\text{C}]{\text{cat. 5, 4 atm H}_2} \text{CH}_3\text{CH}_2\text{-R}$ TOF (mol/h)			
 Ar = 2,6- <i>i</i> -Pr <sub>2</sub> -C <sub>6</sub> H <sub>3</sub> R = H: <b>5</b> , Ph: <b>10</b>			
Substrate			
 1814 <sup>[27]</sup> , [3300] <sup>a [31]</sup> For <b>10</b> : [5300] <sup>a [31]</sup>	 363 <sup>[27]</sup>	 1344 <sup>[27]</sup>	 104 <sup>[27]</sup>
 57 <sup>[27]</sup> , [1075] <sup>a [31]</sup> For <b>10</b> : [60] <sup>a [31]</sup>	 104 <sup>[27]</sup> , [1085] <sup>a [31]</sup> For <b>10</b> : [275] <sup>a [31]</sup>	 3.3 <sup>[27]</sup>	
 3 <sup>[30]</sup>	 320 <sup>[30]</sup>	 1270 <sup>[30]</sup>	 1270 <sup>[30]</sup>
 > 240 <sup>[30]</sup>	 > 240 <sup>[30]</sup>	 > 480 <sup>[30]</sup>	
 19 <sup>c [30]</sup>	 0 <sup>c [30]</sup>	 0.04 <sup>[30]</sup>	 0 <sup>[30]</sup>
 240 <sup>[30]</sup>	 0.4 <sup>[30]</sup>	 > 240 <sup>[30]</sup>	
 4.4 <sup>[30]</sup>	 > 240 <sup>[30]</sup>	 > 240 <sup>[30]</sup>	 > 240 <sup>[30]</sup>

<sup>a</sup>In brackets the results in pentane.<sup>b</sup>The product is (+)-*p*-meth-1-ene.<sup>c</sup>Reaction carried out at 65 °C**Scheme 5** Overreduction of alkynes



**Fig. 3** Substrates leading to decomposition of catalyst **5**

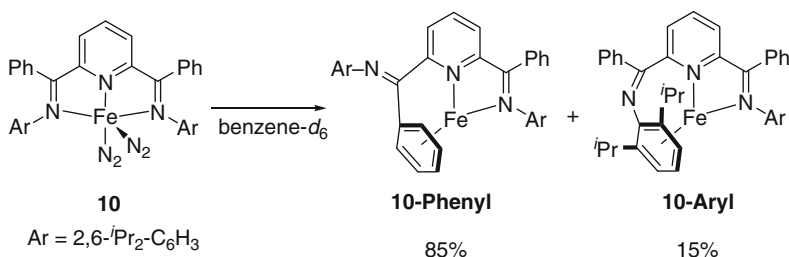
The proposed catalytic cycle, which is based on experimental data, is shown in Scheme 6. Loss of 2 equiv. of  $N_2$  from **5** (or alternatively 1 equiv. of  $N_2$  or 1 equiv. of  $H_2$  from complexes shown in Scheme 3) affords the active species **a**. Olefin coordination giving **b** is considered to be preferred over oxidative addition of  $H_2$ . Then, oxidative addition of  $H_2$  to **b** provides the olefin dihydride intermediate **c**. Olefin insertion giving **d** and subsequent alkane reductive elimination yields the saturated product and regenerates the catalytically active species **a**.



**Scheme 6** Proposed mechanism for catalytic hydrogenation of olefin with **5**

Further investigations revealed that this hydrogenation is accelerated in pentane solution. These results are shown in brackets in Table 3 [31]. Under optimized reaction conditions high catalyst TOF up to 5,300 were achieved when **10** was used. In the absence of both hydrogen and nitrogen, **10** was converted into the  $\eta^6$ -arene complexes such as the bis(imino)pyridine iron  $\eta^6$ -phenyl complex, **10-Phenyl**, and the corresponding  $\eta^6$ -2,6-diisopropylphenyl complex, **10-Aryl**, in the 85:15 ratio in

C<sub>6</sub>D<sub>6</sub> solution (Scheme 7). Both  $\eta^6$ -arene complexes were also determined by the X-ray diffraction and showed no reaction to hydrogen and olefins. Therefore, it was considered that the formation of the  $\eta^6$ -arene complexes was a deactivation pathway in the catalytic hydrogenation.

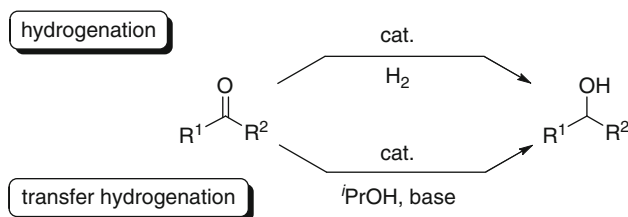


**Scheme 7** Intramolecular arene coordination in bis(imino)pyridine iron complex **10**

## 2.2 Ketone and Aldehyde Reduction

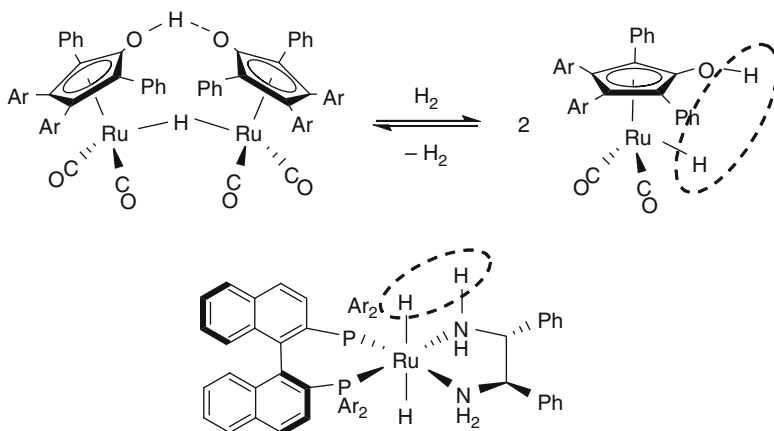
Hydrogenation of substrates having a polar multiple C–heteroatom bond such as ketones or aldehydes has attracted significant attention because the alcohols obtained by this hydrogenation are important building blocks. Usually ruthenium, rhodium, and iridium catalysts are used in these reactions [32–36]. Nowadays, it is expected that an iron catalyst is becoming an alternative material to these precious-metal catalysts.

For transition-metal-catalyzed hydrogenation of ketones and aldehydes, H<sub>2</sub> or the combination of *i*PrOH with a base has been widely used as the hydrogen source (Scheme 8). In case of using H<sub>2</sub>, the reaction is called “hydrogenation,” whereas the reaction using the combination of *i*PrOH with a base is especially called “transfer hydrogenation.”



**Scheme 8** Two pathways of hydrogenation reaction of ketones and aldehydes

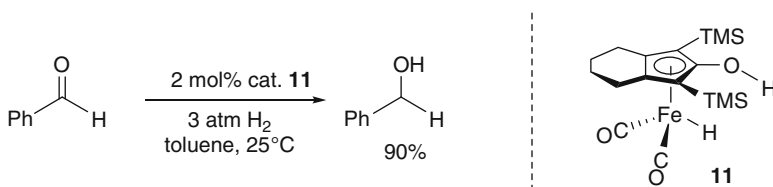
With some transition-metal complexes, the ligand is not only an ancillary ligand. Similar to the transition-metal, it takes directly part in the hydrogen transfer process. Such ligand-metal bifunctional hydrogenation catalysis is dramatically changing the face of reduction chemistry (Scheme 9) (for reviews of ligand-metal bifunctional catalysis, see [32, 37–40]).



**Scheme 9** Examples of ligand-metal bifunctional catalysts

These transition-metal catalysts contain electronically coupled hydridic and acidic hydrogen atoms that are transferred to a polar unsaturated species under mild conditions. The first such catalyst was Shvo's diruthenium hydride complex reported in the mid 1980s [41–44]. Noyori and Ikariya developed chiral ruthenium catalysts showing excellent enantioselectivity in the hydrogenation of ketones [45, 46].

In 2007, Casey showed that **11**, which corresponds to the Shvo's complex catalyzes hydrogenations of ketones and aldehydes [47]. Reaction of benzaldehyde in the presence of catalytic amount of **11** under  $H_2$  (3 atm) afforded the corresponding benzylalcohol in 90% yield within 1 h (Scheme 10).

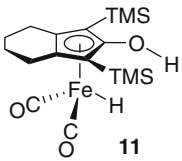
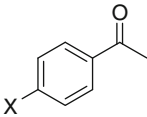
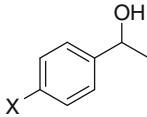
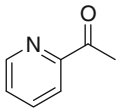
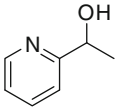
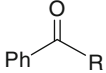
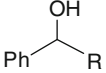
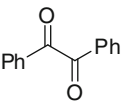
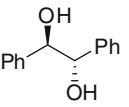
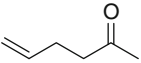
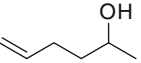
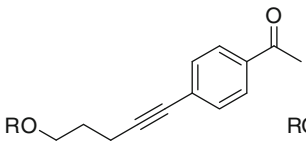
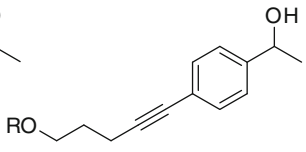


**Scheme 10** Hydrogenation of benzaldehyde catalyzed by complex **11**

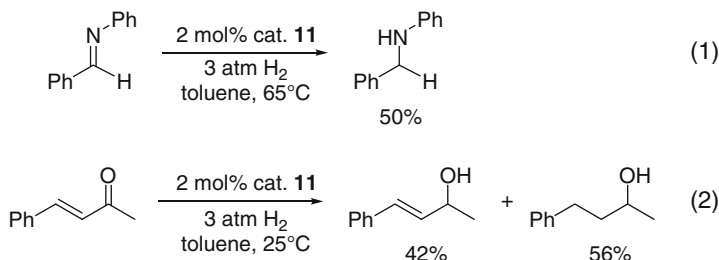
Catalyst **11** showed great tolerance for functional groups like unsaturated carbon–carbon bonds (alkenyl and alkynyl moieties), halides, electron-withdrawing and -donating groups, etc. (Table 4).

Although hydrogenation of *N*-benzylideneaniline in the presence of **11** afforded the corresponding product (eq. 1 in Scheme 11), the  $\alpha,\beta$ -unsaturated ketone was converted into a mixture of unsaturated and saturated alcohols in the 42:56 ratio (eq. 2 in Scheme 11). Several substrates (nitrile derivatives, epoxides, esters, internal alkynes, and terminal alkenes), which are shown in Fig. 4, are not hydrogenated in this catalytic system.

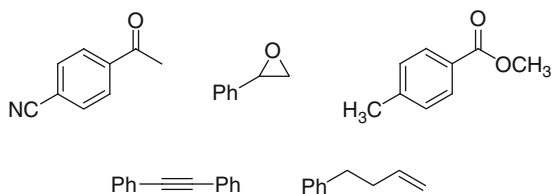
**Table 4** Iron complex-catalyzed hydrogenation of ketones

$R^1-C(=O)-R^2 \xrightarrow[3 \text{ atm } H_2, \text{ toluene, } 25^\circ C]{2 \text{ mol\% cat. } 11} R^1-CH(OH)-R^2$				
Substrate	Product	Yield <sup>a</sup>		
 X = <i>p</i> -H <i>p</i> -Br <i>p</i> -I <i>p</i> -NO <sub>2</sub>		83% (99%) 91% (99%) 84% (99%) 89% (99%)		
		87% (100%)		
 R = Ph CF <sub>3</sub> <i>n</i> -propyl		55% (69%) 91% (100%) 46% (50%)		
		86% (100%) ( <i>meso/dl</i> = 25)		
		87% (100%) <sup>b</sup>		
 R = H CH <sub>2</sub> Ph		57% (71%) 84% (87%)		

<sup>a</sup>Isolated yield (NMR conversion in parentheses).<sup>b</sup>Reaction was performed in diethylether.

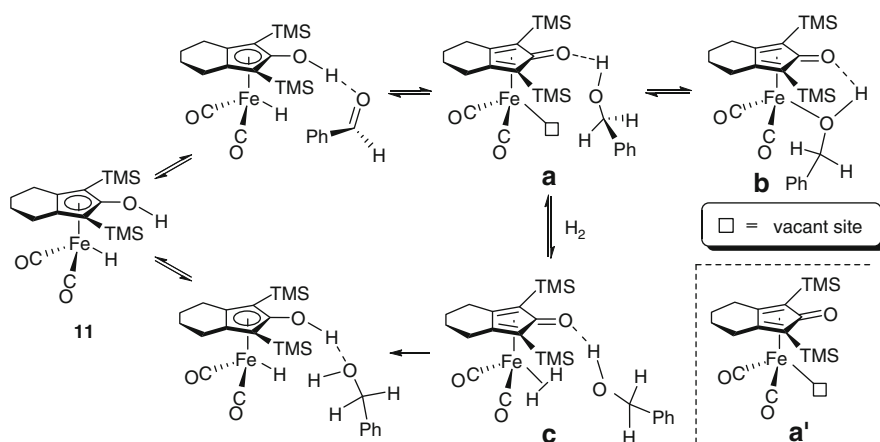


**Scheme 11** Hydrogenation of *N*-benzylideneaniline and  $\alpha,\beta$ -unsaturated ketone catalyzed by complex **11**



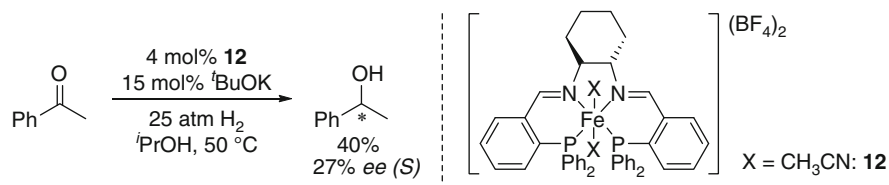
**Fig. 4** Unreacted substrates for hydrogenation catalyzed by **11**

From a mechanistic point of view, this hydrogenation reaction might follow different mechanistic pathways (Scheme 12) [48]. One possibility is that intermediate **a**, which is generated by the transfer of acidic and hydridic hydrogen atoms of **11** to the C=O bond in aldehyde, reacts with H<sub>2</sub> to give dihydrogen complex **c** and then to give the corresponding alcohol and **11**. The second one is that alcohol complex **b** is formed as the initial product and is subsequently converted into **a** which reacts with H<sub>2</sub> to **c**. The subsequent pathway is similar. Finally, it is also possible that the full dissociation of the alcohol from **b** affords intermediate **a'** and then the addition of H<sub>2</sub> to **a'** reproduces **11** to complete the catalytic cycle.



**Scheme 12** Proposed catalytic cycle for Casey's hydrogenation

An iron complex-catalyzed enantioselective hydrogenation was achieved by Morris and coworkers in 2008 (Scheme 13) [49]. Reaction of acetophenone under moderate hydrogen pressure at 50°C catalyzed iron complex **12** containing a tetradentate diiminodiphosphine ligand in the presence of *t*BuOK afforded 1-phenylethanol with 40% conversion and 27% *ee*.



**Scheme 13** Morris' asymmetric hydrogenation catalyzed by iron complex **12**

In addition, the related complexes **13** and **14** act as catalysts in enantioselective transfer hydrogenations (Table 5). The reactivity of acetophenone derivatives

**Table 5** Enantioselective transfer hydrogenation catalyzed by **13** and **14**

$\text{R}^1\text{-CO-R}^2 \xrightarrow[\substack{i\text{PrOH, } 22^\circ\text{C}}]{\substack{0.5 \text{ mol\% } \mathbf{13} \\ 4 \text{ mol\% } t\text{BuOK}}} \text{R}^1\text{-CH(OH)-R}^2$				
Substrate	Time (h)	Conv. (%)	<i>ee</i> (S) (%)	TOF (mol/h)
Ph-CO-Me <sup>a</sup>	0.4	95	29	907
Ph-CO-Me <sup>b</sup>	0.7	33	39	93
Ph-CO-Me	0.4	95	33	454
(2-Cl-C <sub>6</sub> H <sub>4</sub> )-CO-Ph	0.2	>99	18	995
(3-Cl-C <sub>6</sub> H <sub>4</sub> )-CO-Ph	0.4	99	24	495
(4-Cl-C <sub>6</sub> H <sub>4</sub> )-CO-Ph	0.2	94	26	938
(4-Br-C <sub>6</sub> H <sub>4</sub> )-CO-Ph	0.2	93	33	930
(4-Me-C <sub>6</sub> H <sub>4</sub> )-CO-Ph	0.6	86	33	279
(4-OMe-C <sub>6</sub> H <sub>4</sub> )-CO-Ph	0.5	69	23	260
Ph-CO-Et	3.6	95	61	26
C <sub>10</sub> H <sub>7</sub> -CO-Me	0.3	94	25	564
Ph(CH <sub>2</sub> ) <sub>2</sub> -CO-Me	0.6	100	29	315
Ph-CO-Me <sup>c</sup>	2.6	34	76	28

<sup>a</sup>0.25 mol% of **13** and 2 mol% of *t*BuOK were used

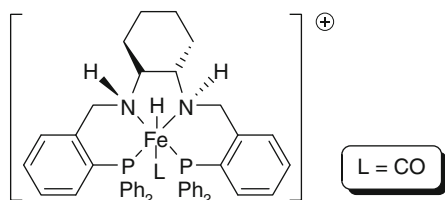
<sup>b</sup>1 mol% of *t*BuOK was used

<sup>c</sup>Reaction catalyzed by **14**

having a *ortho*-halide-substituted aromatic ring is higher. Interestingly, this tendency is opposite to that for the ruthenium-catalyzed transfer hydrogenation reaction reported by Noyori [50]. Catalyst **13** is also efficient for transfer hydrogenations employing diphenylketone, benzaldehyde, or *N*-benzylideneaniline but the *ee* values were not observed. The best enantioselectivity (76% *ee*) was achieved by **14** with acetophenone.

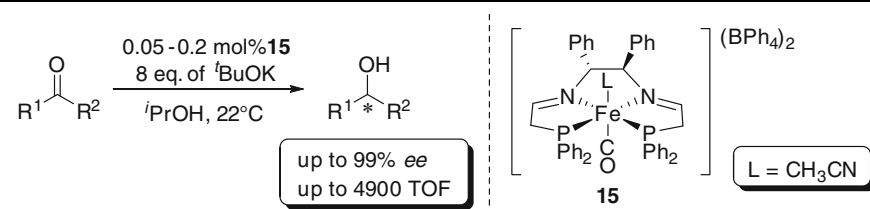
Although details of the mechanism are not clear, it is suggested in analogy to the ruthenium-catalyzed mechanism [51] that the iron hydride complex having amine moieties  $[\text{FeH}(\text{CO})\{(\text{R},\text{R})\text{-PPh}_2(o\text{-C}_6\text{H}_4)\text{CH}_2\text{NHC}_6\text{H}_{10}\text{NHCH}_2(o\text{-C}_6\text{H}_4)\text{PPh}_2\}]^+$ , which is generated by hydrogenation of imine linkage on catalyst **13**, is the candidate for a reactive intermediate (Fig. 5).

**Fig. 5** Proposed catalytic intermediate



A slight modification of the ligand structure finally led to an iron complex **15** with both high catalytic activity and enantiodifferentiation in transfer hydrogenations [52]. Complex **15** acts as an effective catalyst for reduction of functionalized acetophenones containing alkyl groups, cyclic alkanes, chloro- or methoxy-groups on the aryl ring, and others (Table 6). Although the reaction rate is quite low up to 99%, the *ee* value is achieved with 2,2-dimethylpropiophenone. The highest TOF is observed by using 2-aceto-naphtone as substrate. In case of *N*-benzylideneaniline, the *ee* value is not observed.

In 2006, Beller and coworkers demonstrated two Fe-catalyzed transfer hydrogenations of aromatic and aliphatic ketones in the presence of *i*PrONa as a base and *i*PrOH as hydrogen source (Table 7). One is a biomimetic iron porphyrin system [53]. The highest TOF (642) was achieved by in situ generation of the catalyst from  $\text{Fe}_3(\text{CO})_{12}$  and *p*-Cl- $\text{C}_6\text{H}_4$ -substituted porphyrin ligand **L3**. The other catalyst is an iron complex derived from the same iron-source upon combination of terpy and  $\text{PPh}_3$  as ligands in a 1:1 ratio [54]. Other ratios of terpy and  $\text{PPh}_3$ , steric hindered phosphine ligands or bidentate phosphine ligands such as  $\text{Ph}_2\text{P}(\text{CH}_2)_n\text{PPh}_2$  ( $n = 1, 2, 4$ , and 6), and analogous substituted-terpy were not effective. In both protocols, the base plays an important role for the catalytic activity. *i*PrONa and *t*BuONa were efficient, but other inorganic bases, for instance, LiOH and KOH as well as *N*-coordinative organic bases such as pyridine and  $\text{NEt}_3$  showed low activities. In the absence of a base, a transfer hydrogenation was not observed.

**Table 6** Fe-catalyzed transfer hydrogenation of acetophenone

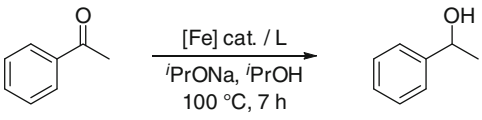
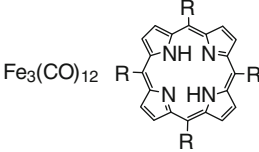
Substrate	Time (min)	Conv. (%)	<i>ee</i> (%)	TOF (mol/h)
Ph-CO-Me	30	90	82	3600
Ph-CO-Me <sup>a</sup>	30	75	84	3000
Ph-CO-Me <sup>b</sup>	30	80	83	3200
Ph-CO-Et	25	90	94	3375
Ph-CO- <sup>t</sup> Bu	200	35	99	53
Ph-CO-( <i>cyclo</i> -C <sub>4</sub> H <sub>7</sub> )	40	95	94	1425
Ph-CO-( <i>cyclo</i> -C <sub>6</sub> H <sub>11</sub> )	85	76	26	536
Ph(CH <sub>2</sub> ) <sub>2</sub> -CO-Me	30	98	14	1960
(4-Cl-C <sub>6</sub> H <sub>4</sub> )-CO-Me	18	96	80	4800
(3-Cl-C <sub>6</sub> H <sub>4</sub> )-CO-Me	13	98	80	4523
(4-MeO-C <sub>6</sub> H <sub>4</sub> )-CO-Me	40	65	54	930
(3-MeO-C <sub>6</sub> H <sub>4</sub> )-CO-Me	30	80	85	2400
<sup>i</sup> Pr-CO-Me	60	86	50	1280
1-Aceto-naphthone	60	93	92	1380
2-Aceto-naphthone	11	90	84	4900
Ph-CH=N-Ph	240	41	—	100

<sup>a</sup>*t*BuONa was used as a base.<sup>b</sup>KOH was used as a base.

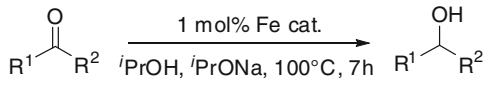
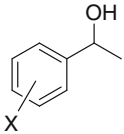
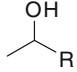
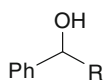
The scope and limitations for transfer hydrogenation employing either the iron porphyrin system or the combination of iron compound/terpy/PPh<sub>3</sub> are listed in Table 8. In most cases, the FeCl<sub>2</sub>/terpy/PPh<sub>3</sub> system displays a higher activity. Except for chloromethyl- and cyclopropyl-acetophenone, the desired products were obtained in good to excellent yields. It should be noted that a ring opened product was not observed when cyclopropyl acetophenone was employed. Hence, a radical-type reduction pathway was excluded and a hydride mechanism appeared to be reasonable.

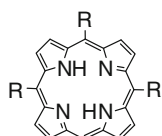
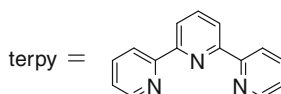
In mechanistic studies, monodeuterated alcohols were obtained by using <sup>i</sup>PrOD (Scheme 14). These results indicate that the intermediate for this transfer hydrogenation was not a dihydride complex but rather a monohydride complex, which was generally accepted by analogous transition-metal-catalyzed reactions [55–57].

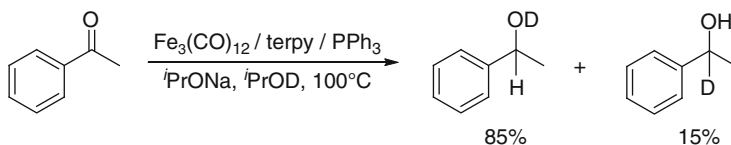
**Table 7** Fe-catalyzed transfer hydrogenation of acetophenone

					
[Fe]	L	Yield(%) <sup>a</sup>	TOF (mol/h) <sup>b</sup>	Ref.	
	R = Ph: <b>L1</b>	93	27	[53]	
	4-pyridyl: <b>L2</b>	94	27	[53]	
	<i>p</i> -Cl-C <sub>6</sub> H <sub>4</sub> : <b>L3</b>	90	26	[53]	
	<b>L3</b>	45 <sup>c</sup>	642 <sup>c</sup>	[53]	
Fe <sub>3</sub> (CO) <sub>12</sub>	terpy / PPh <sub>3</sub>	95		[54]	
FeCl <sub>2</sub>	terpy / PPh <sub>3</sub>	91		[54]	

<sup>a</sup>Yield was determined by GC.<sup>b</sup>Turnover frequencies were determined after 7 h.<sup>c</sup>0.01 mol% of catalyst, which was the one-fiftieth of other iron porphyrin systems, was used.**Table 8** Fe-catalyzed transfer hydrogenation of various ketones<sup>a</sup>

					
Product	L =	Fe <sub>3</sub> (CO) <sub>12</sub>		Fe <sub>3</sub> (CO) <sub>12</sub>	FeCl <sub>2</sub>
		<b>L1</b>	<b>L2</b>	terpy / PPh <sub>3</sub>	
		Yield (%)	Yield (%)	Yield (%)	Yield (%)
	X = <i>p</i> -Cl	93	95	>99	97
	<i>p</i> -Me	50	68	84	83
	<i>p</i> -OMe	46	72	63	75
	<i>o</i> -OMe	>99	>99	>99	>99
	R = Cy	26 [71] <sup>b</sup>	89	95	93
	<sup>t</sup> Bu	11 [55] <sup>b</sup>	90	>99	>99
	R = Et	92	87	81	92
	<sup>c</sup> propyl	21	22	48	57
	CH <sub>2</sub> Cl	<1	<1	5	8

R = Ph: **L1**  
4-pyridyl: **L2**<sup>a</sup>Yield was determined by GC.<sup>b</sup>In brackets the results after 24 h reaction time.



**Scheme 14** Deuterium incorporation into acetophenone catalyzed by  $[\text{Fe}_3(\text{CO})_{12}]/\text{terpy}/\text{PPh}_3/{}^1\text{PrONa}/{}^1\text{PrOD}$  system

The above-described reverse reaction (viz. the Fe-catalyzed dehydrogenation of alcohols to ketones/aldehydes) has been reported by Williams in 2009 (Table 9) [58]. In this reaction, the bicyclic complex **16** shows a sluggish activity, whereas the dehydrogenation of 1-(4-methoxyphenyl)ethanol catalyzed by the phenylated complex **17** affords the corresponding ketone in 79% yield when 1 equiv. (relative to **17**) of  $\text{D}_2\text{O}$  as an additive was used. For this oxidation reaction, 1-(4-methoxyphenyl) ethanol is more suitable than 1-phenylethanol and the reaction rate and the yield of product are higher.

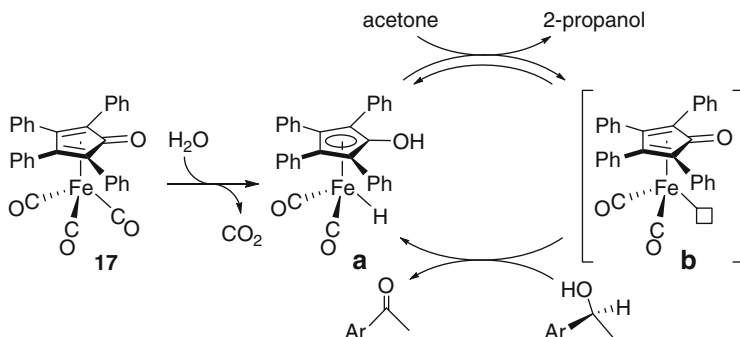
**Table 9** Fe-catalyzed dehydrogen conversion of alcohol to ketone<sup>a</sup>

[Fe]	R	Oxidant	Solvent	T (°C)	Yield%,	Time
<b>16</b> (0.1 equiv.)	H	BQ	$\text{C}_6\text{D}_6$	65	1	16 h
<b>17</b> (0.1 equiv.)	H	BQ	$\text{C}_6\text{D}_6$	65	11	17 h
<b>17</b> (0.1 equiv.)	H	BQ	$\text{C}_6\text{D}_6$	65	24	4 d
<b>17</b> (0.1 equiv.)	OMe	–	$(\text{CD}_3)_2\text{CO}$	54	38	4 d
<b>17</b> (0.2 equiv.) <sup>b</sup>	OMe	–	$(\text{CD}_3)_2\text{CO}$	80	52	4 d
<b>17</b> (0.5 equiv.) <sup>b</sup>	OMe	–	$(\text{CD}_3)_2\text{CO}$	80	79	2 d

<sup>a</sup>Yield was determined by NMR spectroscopy. BQ = benzoquinone.

<sup>b</sup>Experiments were run with 1 equiv. of  $\text{D}_2\text{O}$ .

The proposed catalytic cycle for the dehydrogenation of alcohols to ketones is shown in Scheme 15. The initial reaction of **17** with  $\text{H}_2\text{O}$  affords the hydride complex **a** and  $\text{CO}_2$ . Dehydrogenation of **a** by acetone gives the active species **b** and 2-propanol. The subsequent reaction of **b** with the alcohol yields the corresponding ketone and regenerates **a** to complete the catalytic cycle.



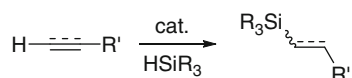
**Scheme 15** Proposed catalytic cycle for dehydrogenation of alcohols to ketones

### 3 Hydrometalation

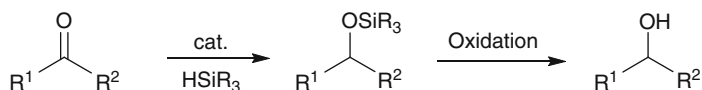
#### 3.1 Hydrosilylation

Organosilicon compounds are widely used in our daily life as oil, grease, rubbers, cosmetics, medicinal chemicals, etc. However, these compounds are not naturally occurring substances but artificially produced ones (for reviews of organosilicon chemistry, see [59–64]). Hydrosilylation reactions catalyzed by a transition-metal catalyst are one of the most powerful tools for the synthesis of organosilicon compounds. Reaction of an unsaturated C–C bond such as alkynes or alkenes with hydrosilane affords a vinyl- or alkylsilane, respectively (Scheme 16).

**Scheme 16** Hydrosilylation of C–C-multiple bonds



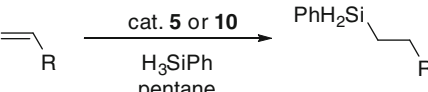
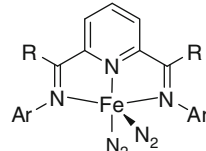
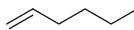
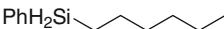
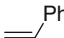
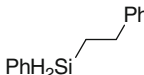
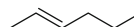
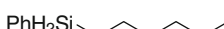
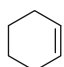
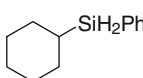
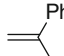
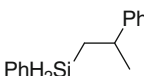

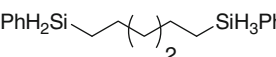
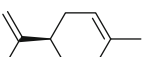
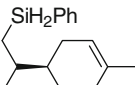
Employing ketones or aldehydes as starting materials, the corresponding silylethers are obtained. Thereafter, the oxidation or hydrolysis of the obtained silylethers gives the corresponding alcohols (Scheme 17). In most cases, a hydride (silyl) metal complex  $\text{H}-\text{M}-\text{Si}$  ( $\text{M}$  = transition-metal), which is generated by an oxidative addition of  $\text{H}-\text{Si}$  bond to the low-valent metal center, is a key intermediate in the hydrosilylation reaction.



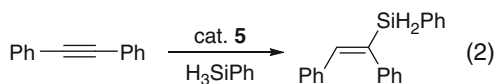
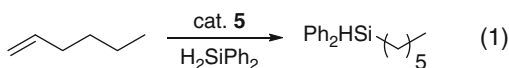
**Scheme 17** Hydrosilylation of carbonyl groups

Bis(imino)pyridine iron complex **5** acts as a catalyst not only for hydrogenation (see **2.1**) but also for hydrosilylation of multiple bonds [27]. The results are summarized in Table 10. The reaction rate for hydrosilylations is slower than that for the corresponding hydrogenation; however, the trend of reaction rates is similar in each reaction. In case of *trans*-2-hexene, the terminal addition product hexyl (phenyl)silane was obtained predominantly. This result clearly shows that an isomerization reaction takes place and the subsequent hydrosilylation reaction delivers the corresponding product. Reaction of 1-hexene with  $\text{H}_2\text{SiPh}_2$  also produced the hydrosilylated product in this system (eq. 1 in Scheme 18). However, the reaction rate for  $\text{H}_2\text{SiPh}_2$  was slower than that for  $\text{H}_3\text{SiPh}$ . In addition, reaction of diphenylacetylene as an alkyne with phenylsilane afforded the monoaddition product due to steric repulsion (eq. 2 in Scheme 18).

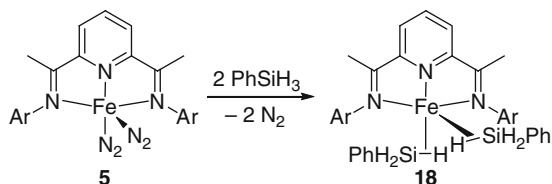
**Table 10** Olefine hydrosilylation catalyzed by **5**

		 Ar = 2,6- <i>i</i> -Pr <sub>2</sub> -C <sub>6</sub> H <sub>3</sub> R = H: <b>5</b> , Ph: <b>10</b>	
Substrate	Product	TOF(mol/h)	
		<b>5</b>	<b>10</b>
		364 <sup>[27]</sup> , 330 <sup>[31]</sup>	930 <sup>[31]</sup>
		242 <sup>[27]</sup>	
		0.09 <sup>a</sup> <sup>[27]</sup>	
		23 <sup>[27]</sup> , 20 <sup>[31]</sup>	16 <sup>[31]</sup>
		104 <sup>[27]</sup>	
		20 <sup>[27]</sup>	
		182 <sup>[27]</sup> , 166 <sup>[31]</sup>	37 <sup>[31]</sup>

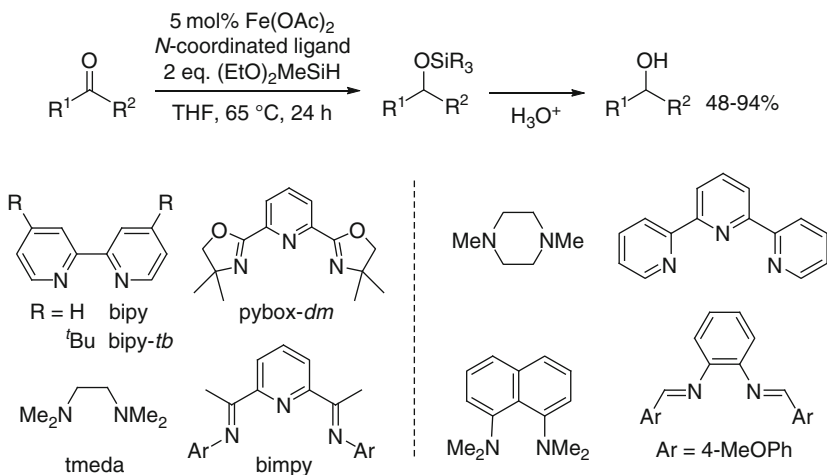
<sup>a</sup>25% of the internal hydrosilylation product was also obtained.

**Scheme 18** Fe-catalyzed hydrosilylation of alkynes and alkenes

Stoichiometric reaction of **5** with phenylsilane produced the iron(0) bis(silane)  $\sigma$ -complex **18**, which was confirmed by the single-crystal X-ray analysis as well as SQUID (Superconducting QUantum Interference Device) magnetometry (Scheme 19). Complex **18** as a precatalyst showed high activity for the hydrosilylation of 1-hexene.

**Scheme 19** Ligand exchange in hydrosilylations

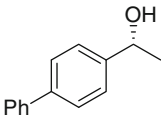
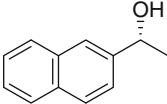
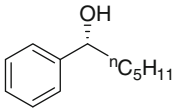
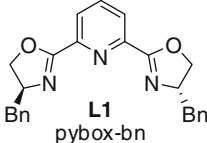
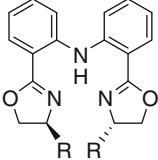
The hydrosilylation of various ketones catalyzed by a combination of  $\text{Fe}(\text{OAc})_2$  with a *N*-coordinated ligand was reported by Nishiyama and Furuta in 2007 [65]. In this reaction, the catalytic activity was dependant on the *N*-coordinated ligands employed (Scheme 20). The ligands on the left side of the dashed line were effective, whereas those on the right side led to no or low catalytic activity.

**Scheme 20** Hydrosilylation of ketones catalyzed by  $\text{Fe}(\text{OAc})_2$  with the *N*-coordinated ligand

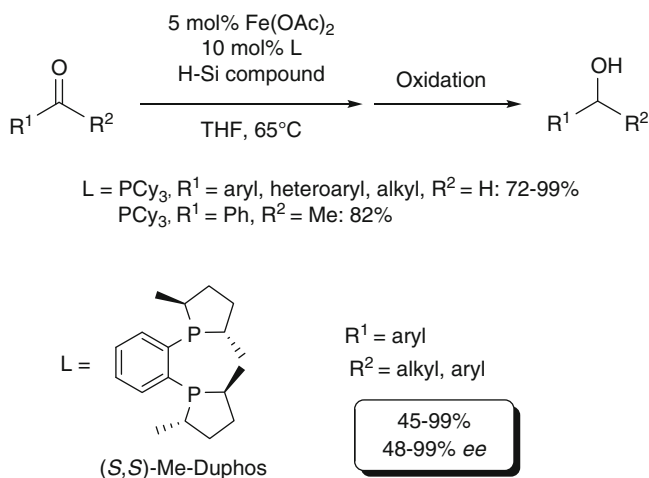
The  $\text{Fe}(\text{OAc})_2/\text{tmeda}$  system showed good activity and chemoselectivity. The bromide and ester groups on the aryl ring of acetophenone were not reduced. Intriguingly, the catalytic activity was improved by using sodium thiophene-2-carboxylate (STC) instead of the *N*-ligand as a ligand for  $\text{Fe}(\text{OAc})_2$  [66]. With the  $\text{Fe}(\text{OAc})_2/\text{STC}$  system, it was possible to use polymethylhydrosiloxane (PMHS) as well as  $(\text{EtO})_2\text{MeSiH}$  as a silyl source. However, in the presence of other iron sources such as  $\text{FeCl}_3$  and  $\text{Fe}(\text{acac})_2$  with STC no hydrosilylation was not observed. In both systems, benzalacetone was reduced to the corresponding alcohol in good to excellent yields with a small amount of 1,4-reduction product. To check the scope of the catalytic reaction of the  $\text{Fe}(\text{OAc})_2/\text{STC}$  system, both transfer hydrogenation and hydrogenation reactions (see 3.2.2) were examined but the system was not very effective.

In 2007, the first asymmetric hydrosilylation was observed when a combination of  $\text{Fe}(\text{OAc})_2$  with the chiral ligand such as a pybox-*bn* (**L1**), bopa-*ip* (**L2**), and bopa-*tb* (**L3**) was used [65]. The results are summarized in Table 11. The best *ee* value (79% (*R*)) was attained by the combination of  $\text{Fe}(\text{OAc})_2$  with **L3**.

**Table 11** The Fe-catalyzed enantioselective hydrosilylation of ketones

$  \begin{array}{c}  \text{R}^1-\text{C}(=\text{O})-\text{R}^2 \xrightarrow[\text{THF, 65}^\circ\text{C}]{\begin{array}{c} 5 \text{ mol\% Fe}(\text{OAc})_2 \\ 7 \text{ mol\% Ligand} \\ 2 \text{ eq. } (\text{EtO})_2\text{MeSiH} \end{array}} \text{R}^1-\text{C}(\text{OSiR}_3)-\text{R}^2 \xrightarrow{\text{H}_3\text{O}^+} \text{R}^1-\text{C}(\text{OH})-\text{R}^2  \end{array}  $			
Product	Ligand	Yield(%)	ee(%)
	<b>L1</b>	93	37 ( <i>R</i> )
	<b>L2</b>	82	57 ( <i>R</i> )
	<b>L3</b>	82	79 ( <i>R</i> )
	<b>L3</b>	59	65 ( <i>R</i> )
	<b>L3</b>	39	59 ( <i>R</i> )
<div style="display: flex; align-items: center; justify-content: space-around;"> <div style="text-align: center;">  <p><b>L1</b> pybox-<i>bn</i></p> </div> <div style="text-align: center;">  <p>R = <sup>i</sup>Pr: <b>L2</b> bopa-<i>ip</i>  <sup>t</sup>Bu: <b>L3</b> bopa-<i>tb</i></p> </div> </div>			

Beller and coworkers reported hydrosilylation reactions of organic carbonyl compounds such as ketones and aldehydes catalyzed by  $\text{Fe}(\text{OAc})_2$  with phosphorus ligands (Scheme 21). In case of aldehydes as starting materials, the  $\text{Fe}(\text{OAc})_2/\text{PCy}_3$  with polymethylhydrosiloxane (PMHS) as an H-Si compound produced the corresponding primary alcohols in good to excellent yields under mild conditions [67]. Use of other phosphorus ligands, for instance,  $\text{PPh}_3$ , bis(diphenylphosphino) methane (dppm), and bis(diphenylphosphino)ethane (dppe) decreased the catalytic activity. It should be noted that *trans*-cinnamaldehyde was converted into the desired alcohol exclusively and 1,4-reduction products were not observed.



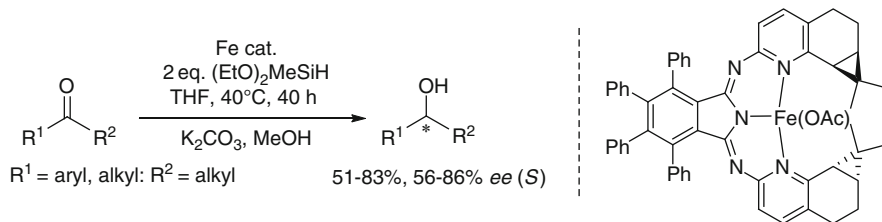
**Scheme 21** Hydrosilylation catalyzed by an Fe complex with phosphorus ligands

An iron complex-catalyzed asymmetric hydrosilylation of ketones was achieved by using chiral phosphorus ligands [68]. Among various ligands, the best enantioselectivities (up to 99% *ee*) were obtained using a combination of  $\text{Fe}(\text{OAc})_2/(\text{S,S})\text{-Me-Duphos}$  in THF. This hydrosilylation works smoothly in other solvents (diethylether, *n*-hexane, dichloromethane, and toluene), but other iron sources are not effective. Surprisingly, this Fe catalyst (45% *ee*) was more efficient in the asymmetric hydrosilylation of cyclohexylmethylketone, a substrate that proved to be problematic in hydrosilylations using Ru [69] or Ti [70] catalysts (43 and 23% *ee*, respectively).

Both Fe-catalyzed systems are compatible with functionalized organic carbonyl compounds such as halides, sterically bulky groups and electron-withdrawing or -donating groups on the aryl ring, or alkyl and heteroaryl groups for aldehydes. A screening of H-Si compounds showed that PMHS and  $(\text{EtO})_2\text{MeSiH}$  were suitable for both reactions.

In 2008, Gade and coworkers reported that the asymmetric hydrosilylation of ketones was catalyzed by the Fe complex with a highly modular class of pincer-type ligand (Scheme 22) [71]. This Fe catalyst system showed both moderate to good

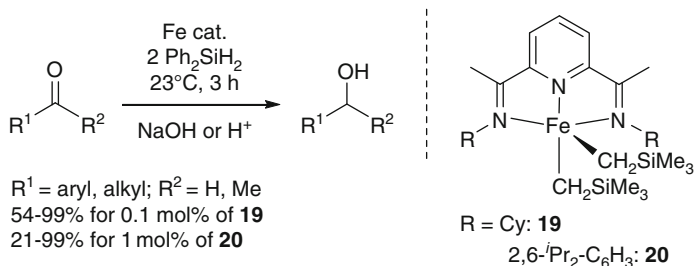
enantioselectivities and yields at slightly elevated temperature. Although the yield of product increased when the reaction was carried out at 65°C, the enantiomeric excess of that decreased. By using sterically bulky dialkyl ketones such as adamantylmethylketone and *t*-butylmethylketone, both yield and enantiomeric excess of products decreased.



**Scheme 22** Asymmetric hydrosilylation catalyzed by the Fe complex with the pincer-type ligand

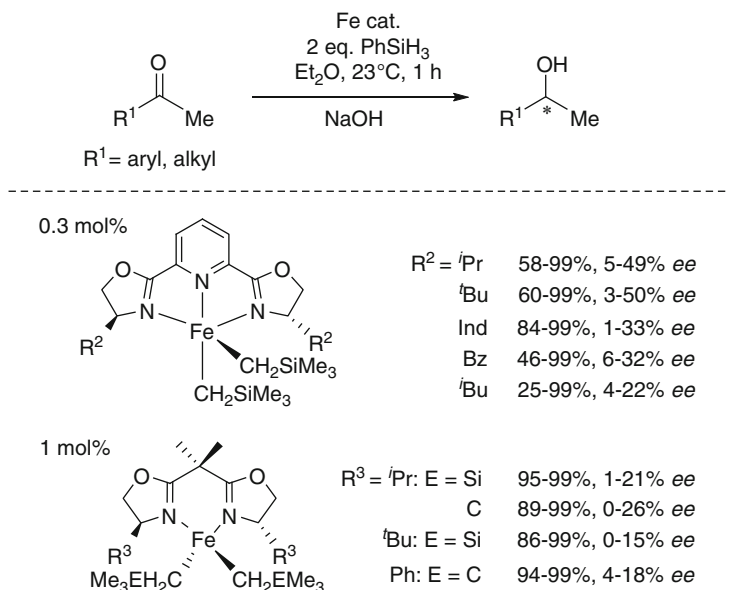
Interestingly, the activity of the corresponding cobalt catalyst possessing a pincer-type ligand is higher than that of the iron complex. In addition, the cobalt complex also acts as a catalyst in asymmetric intermolecular cyclopropanations.

Hydrosilylations of aldehydes and ketones with Ph<sub>2</sub>SiH<sub>2</sub> catalyzed by a bis(imino)pyridine iron complex were also achieved by Chirik and coworkers (Scheme 23) [72]. The catalytic activity of **19** is much higher than that of **20** except using 2-hexanone and 5-hexen-2-one as a ketone. The reaction rate increases with electron-withdrawing groups in the *para* position on the phenyl ring (the order of activity: CF<sub>3</sub> > H > OMe > <sup>*t*</sup>Bu > NMe<sub>2</sub>). This tendency is similar to that observed for the corresponding hydrogenations, which was reported by Morris (see 2.2) [49].



**Scheme 23** Hydrosilylation catalyzed by a bis(imino)pyridine iron complex

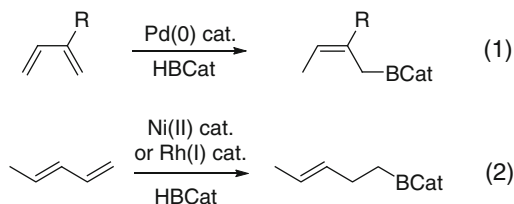
The comparison of a bis(imino)pyridine iron complex and a pyridine bis(oxazoline) iron complex in hydrosilylation reactions is shown in Scheme 24 [73]. Both iron complexes showed efficient activity at 23°C and low to modest enantioselectivities. However, the sterically hindered acetophenone derivatives such as 2',4',6'-trimethylacetophenone and 4'-*tert*-butyl-2',6'-dimethylacetophenone reacted sluggishly. The yields and enantioselectivities increased slightly when a combination of iron catalyst and B(C<sub>6</sub>F<sub>5</sub>)<sub>3</sub> as an additive was used.



**Scheme 24** The comparison of a bis(imino)pyridine iron complex and a pyridine bis(oxazoline) iron complex for hydrosilylation of ketones

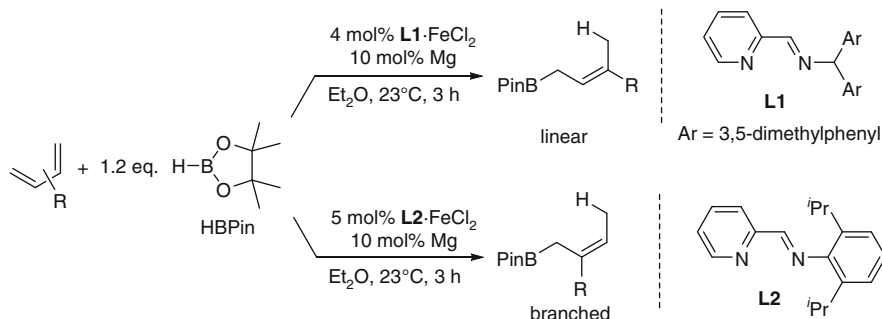
### 3.2 Hydroboration

Allylboranes are widely used in organic synthesis (for recent examples, see [74–82]) and have been prepared mainly by using Grignard and organolithium reagents. However, these conventional methods present shortcomings such as inapplicability for compounds with an electrophilic functional group [75]. Although transition-metal-catalyzed hydroborations of olefins is well-established (for reviews of transition-metal-catalyzed hydroboration, see [83, 84]), examples for hydroborations of dienes are comparably rare. Hence, the Pd(0)-catalyzed hydroboration reaction of unfunctionalized 1,3-dienes with catecholborane affords branched (*Z*)-allylic boronates as a result of a 1,4-addition (eq. 1 in Scheme 25) [85], while Rh(I)- [86] and Ni(II)-catalyzed [87] hydroboration reactions afford 1,2-addition products mainly (eq. 2 in Scheme 25).



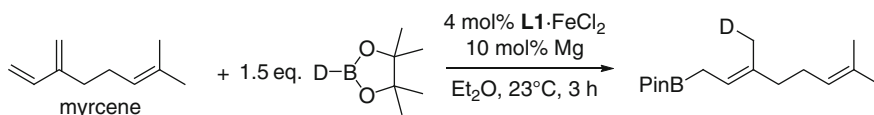
**Scheme 25** Transition metal catalyzed hydroboration of 1,3-dienes

In 2009, Ritter and coworkers reported a selective Fe-catalyzed hydroboration of 1,3-dienes to produce linear (*E*)- $\gamma$ -disubstituted allylboranes under mild conditions when a combination of **L1**·FeCl<sub>2</sub> and magnesium metal as a catalyst was used. The branched (*E*)-allylboranes were obtained by using **L2**·FeCl<sub>2</sub> instead of **L1**·FeCl<sub>2</sub> (Scheme 26) [88]. For the synthesis of 2-borylallylsilanes, this method was superior to the previously reported silaboration of allenes [89].



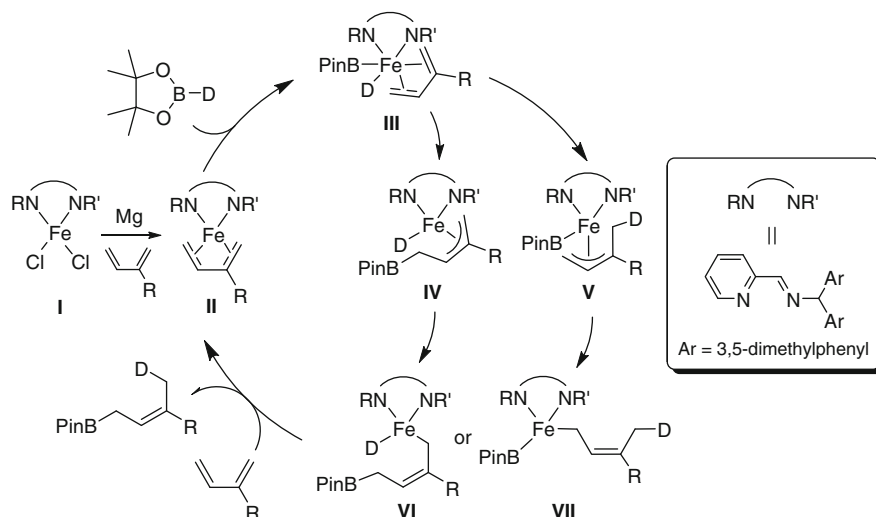
**Scheme 26** 1,4-Hydroboration of 1,3-diene derivatives with pinacolborane catalyzed by an iron complex

For a mechanistic investigation, hydroboration of myrcene with pinacolborane-*d*<sub>1</sub> was examined. A selective deuteration was observed at the methyl group of the hydroboration product (Scheme 27).



**Scheme 27** Selected deuteration in hydroboration of myrcene catalyzed by FeCl<sub>2</sub> with **L1**

The proposed mechanism for Fe-catalyzed 1,4-hydroboration is shown in Scheme 28. The FeCl<sub>2</sub> is initially reduced by magnesium and then the 1,3-diene coordinates to the iron center (**I**  $\rightarrow$  **II**). The oxidative addition of the B–D bond of pinacolborane-*d*<sub>1</sub> to **II** yields the iron hydride complex **III**. This species **III** undergoes a migratory insertion of the coordinated 1,3-diene into either the Fe–B bond to produce  $\pi$ -allyl hydride complex **IV** or the Fe–D bond to produce  $\pi$ -allyl boryl complex **V**. The  $\pi$ – $\sigma$  rearrangement takes place (**IV**  $\rightarrow$  **VI**, **V**  $\rightarrow$  **VII**). Subsequently, reductive elimination to give the C–D bond from **VI** or to give the C–B bond from **VII** yields the deuterated hydroboration product and reinstalls an intermediate **II** to complete the catalytic cycle. However, up to date it has not been possible to confirm which pathway is correct.



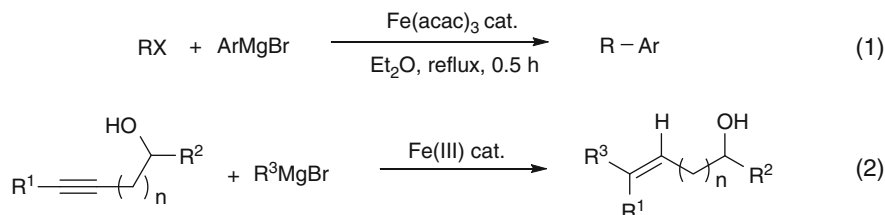
**Scheme 28** Proposed mechanism for 1,4-hydroboration

## 4 Organic Synthesis

### 4.1 C–C and C–E Bond Formation

C–C and C–E (E = heteroatom) bond formations are valuable reactions in organic synthesis, thus these reactions have been achieved to date by considerable efforts of a large number of chemists using a precious-metal catalysts (e.g., Ru, Rh, and Pd). Recently, the application range of iron catalysts as an alternative for rare and expensive transition-metal catalysts has been rapidly expanded (for recent selected examples, see [12–20, 90–103]). In these reactions, a Fe–H species might act as a reactive key intermediate but also represent a deactivated species, which is prepared by  $\beta$ -H elimination.

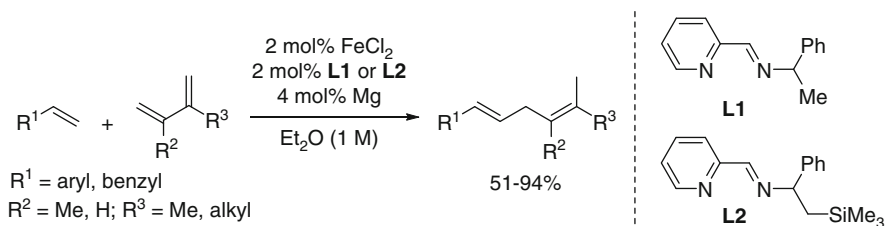
Iron-catalyzed cross-coupling reaction of aryl Grignard reagents with alkyl halides possessing  $\beta$ -hydrogens was achieved by Hayashi and Nagano in 2004 (eq. 1 in Scheme 29) [104]. Although alkyl Grignard reagents with aryl and alkyl halides do not fit in this reaction, the combination of secondary alkyl halides as well as primary ones with aryl Grignard reagents are adaptable. In 2006, Ready and Zhang reported that the carbometallation-cross coupling of propargylic and homo-propargylic alcohols affords tri- and tetrasubstituted olefins with high regio- and stereo-selectivity catalyzed by Fe(III) complexes such as  $\text{Fe}(\text{acac})_3$  and  $\text{Fe}(\text{ehx})_3$  (ehx = 2-ethylhexanoate) (eq. 2 in Scheme 29) [105]. While Cu(I) salts show a low activity (<5% conversion) [106, 107],  $\text{Co}(\text{OAc})_2$  and  $\text{Ni}(\text{acac})_2$  catalysts afford the corresponding products in moderate yields.



**Scheme 29** Iron-catalyzed cross coupling reaction of aryl Grignard reagents with alkyl halides

The initially formed tetra-alkylferrate(II) represents the reactive intermediate in both reactions that undergoes a carboferration of the triple bond in eq. 2, Scheme 29. Transmetalation from Fe to Mg yields a vinyl-magnesium species, which liberates the desired olefin upon hydrolysis within the acidic work-up procedure. In the above two reactions, a competing  $\beta$ -hydride elimination from the ferrate yields the unreactive Fe–H species and hence is considered to be the deactivation step in the catalytic cycle.

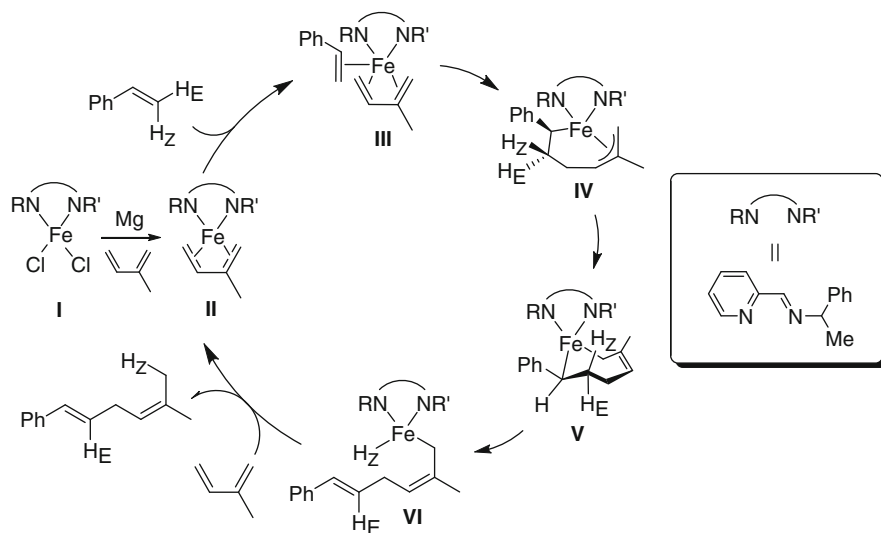
In 2009, Ritter and coworkers reported a stereo- and regio-selective 1,4-addition of  $\alpha$ -olefins to 1,3-dienes catalyzed by the mixture of  $\text{FeCl}_2$ , the iminopyridine ligand (**L1** or **L2**), in the presence of magnesium metal (Scheme 30) [108]. This combination is also adaptable to the 1,4-hydroboration of 1,3-dienes (see 3.2).



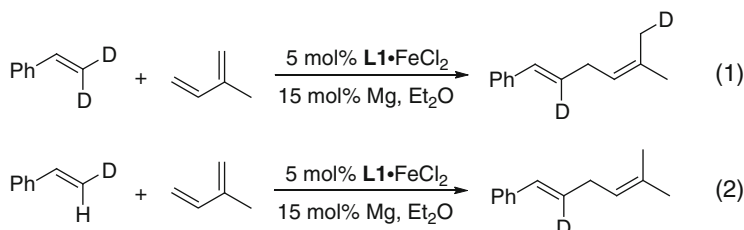
**Scheme 30** Fe-catalyzed 1,4-addition of  $\alpha$ -olefins to 1,3-dienes

In contrast to the hydroboration protocol, this reaction affords the linear 1,4-diene addition products in either case as the sole product using both **L1** or **L2** as a ligand. The system possesses a good degree of functional group tolerance for the functionalized styrenes with electron-withdrawing or -donating groups such as halides, ethers, and esters on the aryl ring.

The proposed catalytic cycle is shown in Scheme 31. Hence,  $\text{FeCl}_2$  is reduced by magnesium and subsequently coordinates both to the 1,3-diene and  $\alpha$ -olefin (**I**  $\rightarrow$  **III**). The oxidative coupling of the coordinated 1,3-diene and  $\alpha$ -olefin yields the allyl alkyl iron(II) complex **IV**. Subsequently, the  $\pi$ – $\sigma$  rearrangement takes place (**IV**  $\rightarrow$  **V**). The *syn*- $\beta$ -hydride elimination ( $\text{H}_Z$ ) gives the hydride complex **VI** from which the C–H $\beta$  bond in the 1,4-addition product is formed via reductive elimination with regeneration of the active species **II** to complete the catalytic cycle. Deuteration experiments support this mechanistic scenario (Scheme 32).

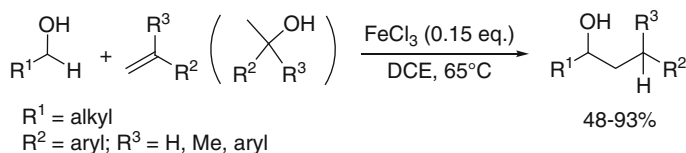


**Scheme 31** Fe-catalyzed 1,4-addition of  $\alpha$ -olefins to 1,3-dienes



**Scheme 32** Deuteration experiment for 1,4-addition of  $\alpha$ -olefins to diene catalyzed by an iminopyridine-ferrous chloride complex

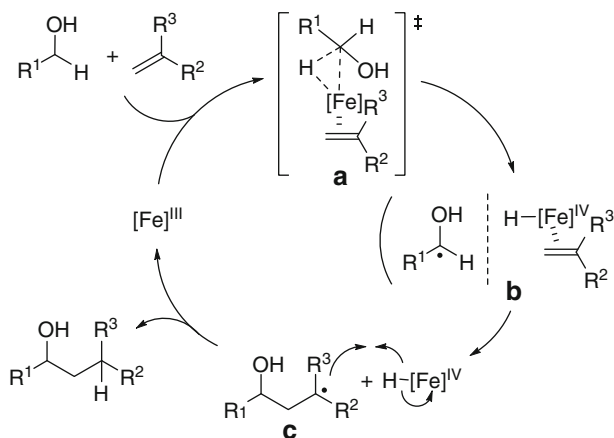
Iron-catalyzed  $C(sp^3)-C(sp^3)$  bond-forming cross-coupling reactions of alcohols with alkenes has been reported by Tu and coworkers in 2009 [109]. Reactions of primary alcohols with various alkenes in the presence of a catalytic amount of  $FeCl_3$  in 1,2-dichloroethane afford the desired secondary alcohols as the cross-coupling products in moderate to good yields (Scheme 33). Iron sources such as



**Scheme 33** Fe-catalyzed primary alcohols with various alkenes

$\text{FeCl}_2$ ,  $\text{Fe}(\text{acac})_3$ , and  $\text{Fe}(\text{ClO}_4)_3$  instead of  $\text{FeCl}_3$ , however, showed low activity. Tertiary alcohols, such as 3-phenylpropanol or cyclohexylmethanol instead of alkenes, are also adaptable to this reaction.

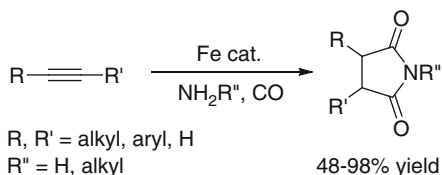
Based upon deuterium-labeling experiments, the following catalytic cycle was proposed (Scheme 34). The Fe(III) center coordinates to the olefin and interacts with the  $\text{C}(\text{sp}^3)\text{--H}$  bond adjacent to the oxygen atom of the alcohol to form intermediate **a**. Cleavage of the  $\text{C}(\text{sp}^3)\text{--H}$  bond gives radical pair **b**. Subsequently, both free-radical addition and dissociation afford a free-radical and a Fe(IV)–H species. The hydrogen transfer from the hydride complex to **c** gives the desired product and regenerates the  $[\text{Fe}]^{\text{III}}$  catalyst for the next catalytic cycle.



**Scheme 34** Proposed catalytic cycle for the C–C bond formation

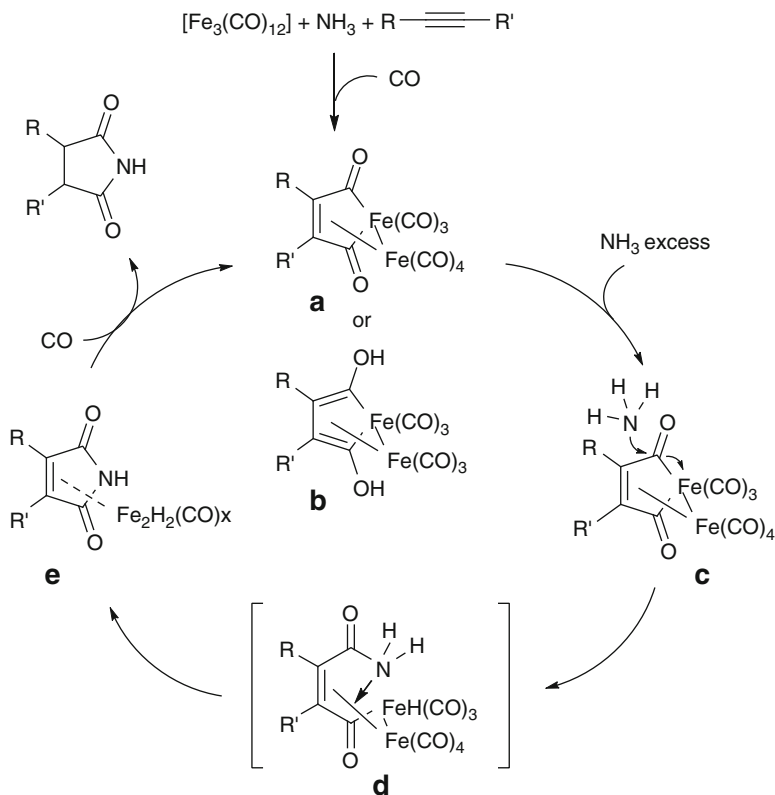
Beller and coworkers found in 2009 that alkynes react with amines under the CO pressure (20 bar) in the presence of catalytic amounts of  $[\text{Fe}_3(\text{CO})_{12}]$  to the corresponding succinimide in moderate to excellent yields (Scheme 35) [110]. Various terminal and internal alkynes and ammonia or primary amines are adaptable for this transformation. Furthermore,  $[\text{Fe}(\text{CO})_5]$  as an iron source showed high activity. The catalytic activity, however, decreased considerably when a phosphine ligand such as  $\text{PPh}_3$  and  $(^t\text{Bu})_2\text{P}(\text{''Bu})$  was employed.

**Scheme 35** Synthesis of succinimides catalyzed by an iron complex



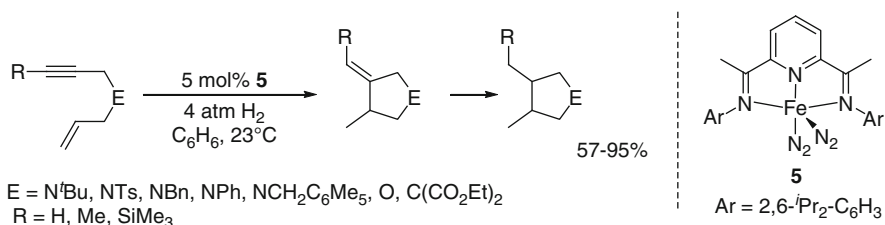
The proposed reaction mechanism, which is assisted by Periasamy's stoichiometric reaction [111–118], is shown in Scheme 36. Initially, the reaction of  $[\text{Fe}_3(\text{CO})_{12}]$

with an amine gives both an “amine- $[\text{Fe}(\text{CO})_4]$ ” and an  $[\text{Fe}_2(\text{CO})_8]$  species. Subsequently,  $[\text{Fe}_2(\text{CO})_8]$  reacts with alkynes under CO pressure to yield complexes **a** or **b**. The corresponding cyclic imides are obtained by the reaction of **a** or **b** with an excess amount of amine and CO via intermediates **c**–**d**. Although some mechanistic details are unapparent, hydride complex **d** and dihydrogen complex **e** are considered to be key intermediates.



**Scheme 36** Reaction mechanism of the formation of succinimides catalyzed by iron complexes

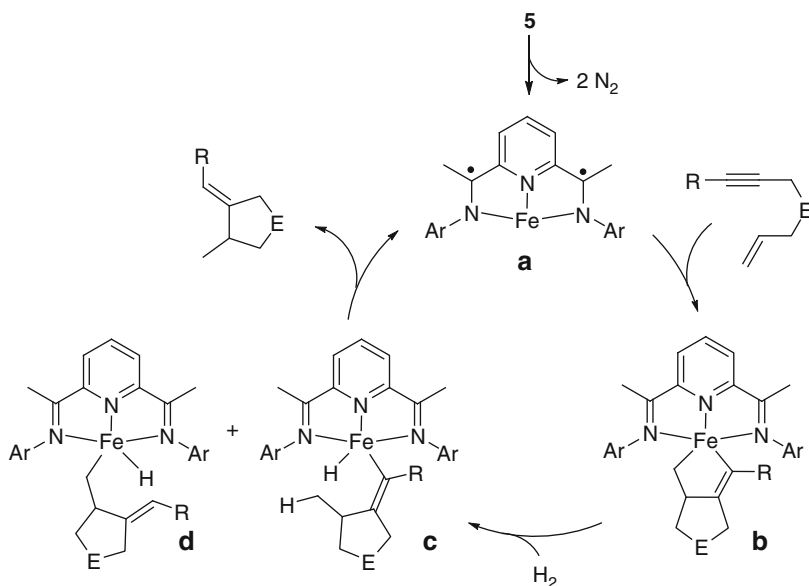
In 2009, Chirik reported a hydrogen-mediated reductive enyne cyclization catalyzed by the bis(imino)pyridine iron complex **5** (Scheme 37) [119]. In the



**Scheme 37** Synthesis of succinimides catalyzed by an iron complex

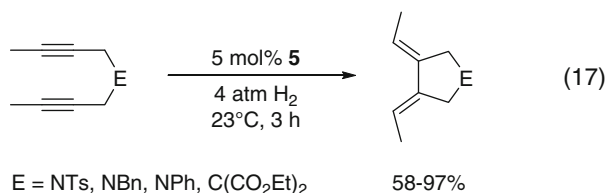
presence of the Fe catalyst under hydrogen pressure, various 1,6-enynes are readily converted into the corresponding cyclic products. The unsaturated moiety on the product is subsequently hydrogenated to give the desired products such as pyrrolidine, tetrahydrofuran, and cyclopentane derivatives (see also 3.2.1) [120].

The catalytic cycle, which is supported by stoichiometric and labeling experiments, is shown in Scheme 38. Loss of 2 equiv. of  $N_2$  from **5** affords the active species **a**. Reaction of **a** with the 1,6-enyne gives the metallacycle complex **b**. Subsequently, **b** reacts with  $H_2$  to give the alkenyl hydride complex **c** or the alkyl hydride complex **d**. Finally, reductive elimination constructs the C–H bond in the cyclization product and regenerates intermediate **a** to complete the catalytic cycle.



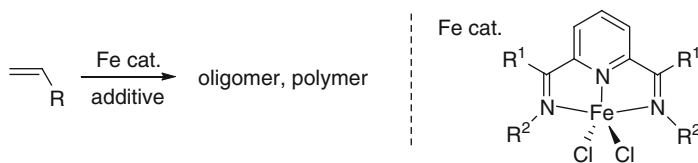
**Scheme 38** Catalytic cycle for the hydrogen-mediated enyne cyclization

In addition, (Z,Z)-3,4-diethylene-substituted pyrrolidines and cyclopentane are obtained when 2,7-diyne were used as a starting material in Scheme 39.



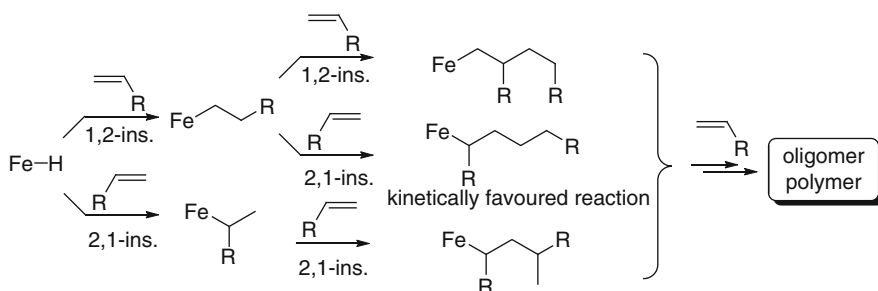
**Scheme 39** Reductive cyclization of diynes

As an alternative method for the C–C bond formation, oligomerization and polymerization reactions of olefins catalyzed by a bis(imino)pyridine iron complex are also well known (Scheme 40) [121–124].



**Scheme 40** Olefin polymerization catalyzed by a bis(imino)pyridine iron complex

The corresponding iron-catalyzed oligomerization of ethylene was developed by Gibson and coworkers [125]. A combination of an iron precatalyst with MAO (methyl aluminoxane) yields a catalyst that affords ethylene oligomers (>99% linear  $\alpha$ -olefin mixtures). The activity of ketimine iron complexes ( $R^1 = \text{Me}$ ) is higher than that of the aldimine analogs ( $R^1 = \text{H}$ ) and also the  $\alpha$ -value of the oligomer is better (Scheme 41).



**Scheme 41** The proposed mechanism of olefin polymerization

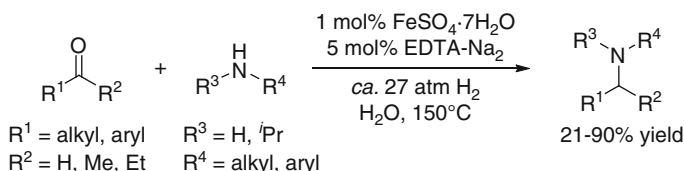
A head-to-head dimerization of  $\alpha$ -olefin catalyzed by a bis(imino)pyridine iron complex has been reported by Small and Marcucci [126]. This reaction delivers linear internal olefins (up to 80% linearity) from  $\alpha$ -olefins. The linearity of products, however, depends on the catalyst structure and the reaction conditions.

Fink and Babik reported that propylene polymerization was achieved by a bis(imino)pyridine iron complex with  $\text{Ph}_3\text{C}[\text{B}(\text{C}_6\text{F}_5)_4]$  and trialkylaluminium as additives [127]. Both 3-methyl- $n$ -butyl and  $n$ -butyl endgroups were observed by  $^{13}\text{C}$  NMR spectrum when triisobutylaluminium as an activator was used, whereas the only  $n$ -propyl endgroup was formed in case of triethylaluminium activation. In addition, this polymerization proceeds two times faster with than without a hydrogen atmosphere, but the  $M_n$  value decreases and the  $M_w/M_n$  value rises up.

The reaction mechanism is investigated by using DFT calculations [128, 129] indicating formation of a Fe–H species to be an important step. In case of 1-butene, the synthesis

of linear octenes (i.e., 1,2- and the successive 2,1-insertions of 1-butene) is kinetically favored rather than that of branched products (Scheme 41). Dimers are obtained via a competitive reaction of  $\beta$ -hydrogen elimination and  $\beta$ -hydrogen transfer termination. Further insertion reaction into the Fe-C bond affords higher oligomers and polymers.

The direct reductive amination (DRA) is a useful method for the synthesis of amino derivatives from carbonyl compounds, amines, and  $H_2$ . Precious-metal (Ru [130–132], Rh [133–137], Ir [138–142], Pd [143]) catalyzed reactions are well known to date. The first Fe-catalyzed DRA reaction was reported by Bhanage and coworkers in 2008 (Scheme 42) [144]. Although the reaction conditions are not mild (high temperature, moderate  $H_2$  pressure), the hydrogenation of imines and/or enamines, which are generated by reaction of organic carbonyl compounds with amines, produces various substituted aryl and/or alkyl amines. A dihydrogen or dihydride iron complex was proposed as a reactive intermediate within the catalytic cycle.



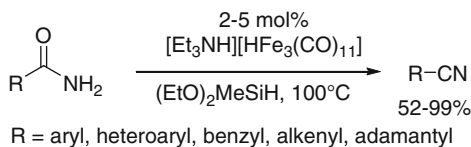
**Scheme 42** Direct reductive amination of organic carbonyl compounds

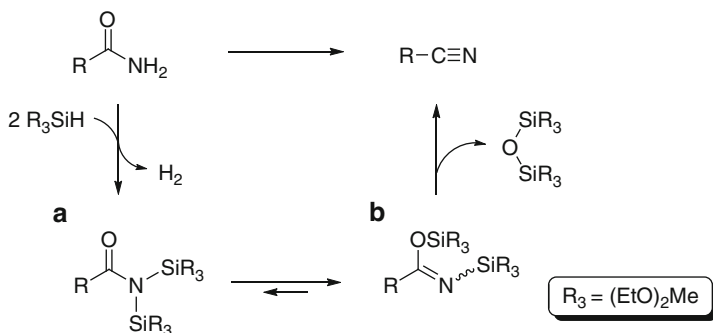
## 4.2 Others

The dehydration of primary amides with hydrosilane catalyzed by iron carbonyl clusters, such as  $[\text{Et}_3\text{NH}][\text{HFe}_3(\text{CO})_{11}]$  and  $\text{Fe}_2(\text{CO})_9$ , was achieved by Beller and coworkers in 2009 (Scheme 43) [145]. This reaction shows good functional group tolerance (e.g., such as aromatic, heteroaromatic, and aliphatic substrates).

A mechanistic proposal, which is based on the ruthenium-catalyzed dehydration reaction reported by Nagashima and coworkers [146], is shown in Scheme 44. Reaction of a primary amine with hydrosilane in the presence of the iron catalyst affords the bis(silyl)amine **a** and 2 equiv. of  $H_2$ . Subsequently, the isomerization of **a** gives the *N,O*-bis(silyl)imide **b** and then elimination of the disiloxane from **b** produces the corresponding nitrile. Although the disiloxane and its monohydrolysis product were observed by  $^{13}\text{C}$  and  $^{29}\text{Si}$  NMR spectroscopy and by GC-Mass-analysis, intermediates **a** and **b** were not detected.

**Scheme 43** Fe-catalyzed dehydration of amides to nitriles

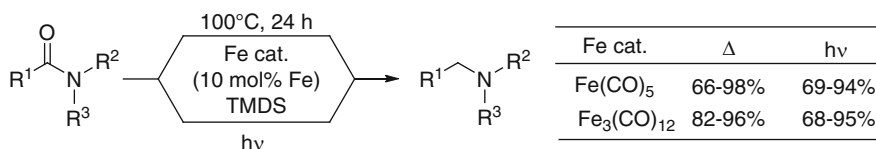
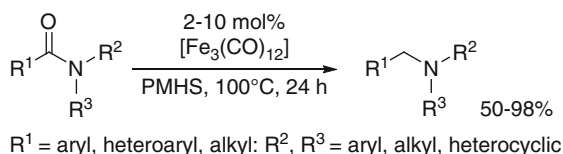




**Scheme 44** Plausible pathway of Fe-catalyzed dehydration of primary amides to nitriles

In 2009, Beller (Scheme 45) [147] and Nagashima (Scheme 46) [148] independently reported an iron-catalyzed hydrosilane reduction of carboxamides to amines. Although inexpensive PMHS and TMDS as an H–Si source are usable, the yield of product considerably decreased when hydrosilane containing only one H–Si moiety or iron sources such as  $\text{Fe}(\text{acac})_2$  and  $\text{FeX}_2$  ( $\text{X} = \text{F}, \text{Cl}$ ) was used. In both thermal and photoassisted conditions, almost the same reactivities were observed upon using a combination of Fe catalyst with TMDS (Scheme 46).

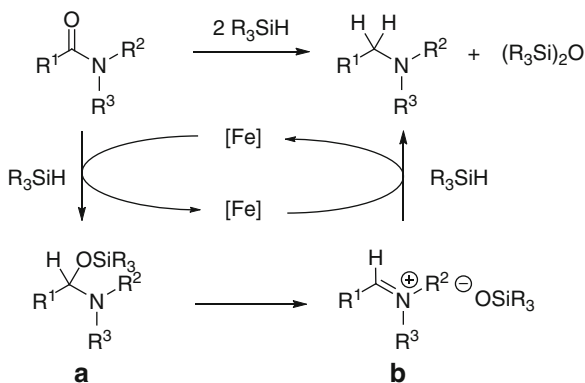
**Scheme 45** Fe-catalyzed deduction of amides to amines



$R^1 = \text{aryl, alkyl}; R^2, R^3 = \text{alkyl, heterocyclic}$

**Scheme 46** Fe-catalyzed reduction of amides to amines under either thermal or photoassisted conditions

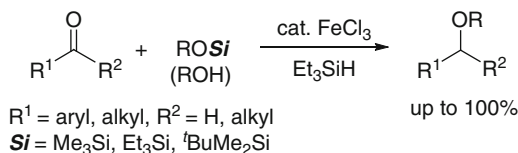
A catalytic mechanism, which is supported by deuterium-labeling experiments in the corresponding Ru-catalyzed procedure [146], is shown in Scheme 47. Accordingly, the reactive Fe-hydride species is formed in situ by the reaction of the iron precatalyst with hydrosilane. Hydrosilylation of the carboxyl group affords the *O*-silyl-*N,O*-acetal **a**, which is converted into the iminium intermediate **b**. Reduction of **b** by a second Fe-hydride species finally generates the corresponding amine and disiloxane.



**Scheme 47** Fe-catalyzed hydrosilane reduction of amides to amines

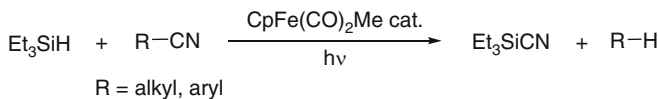
Oriyama and coworkers reported an iron-catalyzed reductive etherification of carbonyl compounds with triethylsilane and alkoxytrialkylsilane [149, 150] and alcohols (Scheme 48) [151].

**Scheme 48** Iron-catalyzed reductive etherification of carbonyl compounds



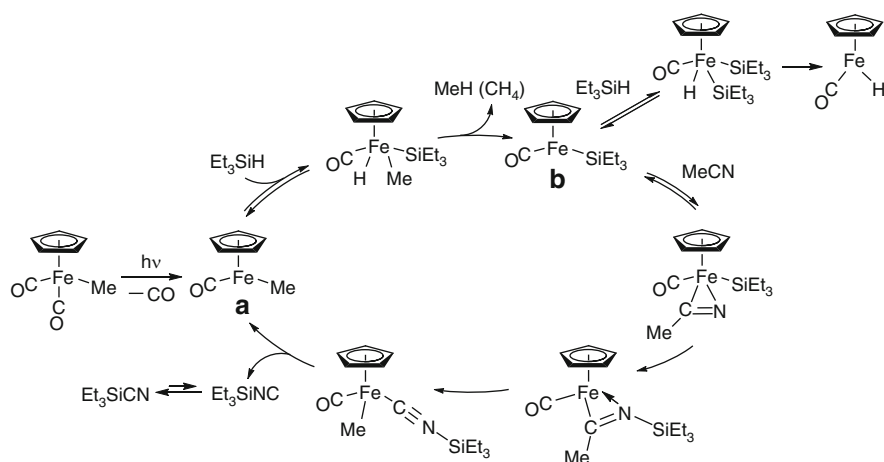
Although some methods for reductive etherifications of carbonyl compounds have been reported [152–162], the iron-catalyzed version possesses several advantages: (1) fairly short reaction times are needed, (2) not only trimethylsilyl ether but also triethylsilyl and *t*-butyldimethylsilyl ethers and alcohols are adaptable, and (3) a broad substrate scope.

Our groups developed a catalytic C–CN bond cleavage of organonitriles catalyzed by the Fe complex (Scheme 49) [163, 164]. In this reaction, an organonitrile R–CN and Et<sub>3</sub>SiH are converted into Et<sub>3</sub>SiCN as a result of the C–CN bond cleavage and the Si–CN bond formation, and the R–H product. This is the first example of the catalytic C–CN bond cleavage of acetonitrile.



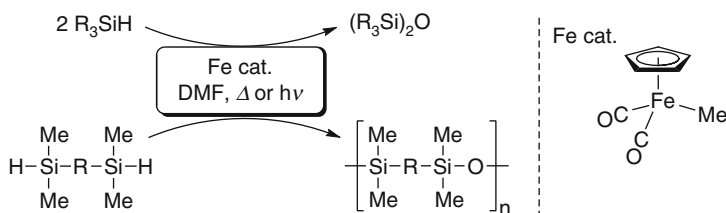
**Scheme 49** Iron-catalyzed decyanation of nitriles

Supported by DFT calculation [165], we proposed the mechanism shown in Scheme 50 for the reaction with acetonitrile. Thus, one CO ligand in  $\text{CpFe}(\text{CO})_2\text{Me}$  is released via photolysis to give the 16-electron species **a**  $\text{CpFe}(\text{CO})\text{Me}$ . In the presence of  $\text{Et}_3\text{SiH}$ , the hydride complex  $\text{CpFe}(\text{CO})\text{Me}(\text{H})(\text{SiEt}_3)$  is formed. Subsequently, reductive elimination to give  $\text{CH}_4$  yields the important intermediate **b**  $\text{CpFe}(\text{CO})(\text{SiEt}_3)$ , which reacts with  $\text{R-CN}$  to give  $\text{CpFe}(\text{CO})(\text{SiEt}_3)(\eta^2\text{-NCR})$ . This nitrile complex is then converted into  $\text{CpFe}(\text{CO})(\text{Me})(\eta^1\text{-CNSiEt}_3)$ . Finally, dissociation of  $\text{Et}_3\text{SiNC}$  regenerates **a** to complete the catalytic cycle. The released  $\text{Et}_3\text{SiNC}$  isomerizes to  $\text{Et}_3\text{SiCN}$ . In addition to the reaction of **b** with  $\text{MeCN}$ , **b** reacts also with  $\text{Et}_3\text{SiH}$  to give the bis(silyl)hydride complex, which is isolable.



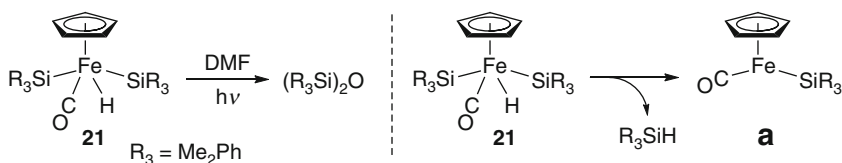
**Scheme 50** Fe-catalyzed the C-CN bond cleavage of acetonitrile

We also reported that  $\text{CpFe}(\text{CO})_2\text{Me}$  acts as a precursor for the Si-O-Si bond formation reaction from hydrosilane and DMF (Scheme 51) [166, 167]. In this reaction, tertiary silanes and bis(silyl) compounds are converted into the corresponding disiloxanes and the polymers with  $(\text{-R-Si-O-Si-})_n$  backbone, respectively.



**Scheme 51** The Fe-catalyzed Si-O-Si bond formation reaction from hydrosilanes and DMF

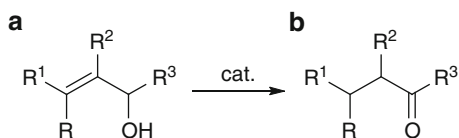
The reaction of  $\text{CpFe(CO)}_2\text{Me}$  with  $\text{R}_3\text{SiH}$  gives the bis(silyl)hydride complex **21**. Photoreaction of **21** in DMF afforded the corresponding disiloxane (Scheme 52). We believe that the oxygen in the disiloxane is derived from DMF, because  $\text{NMe}_3$  is concomitantly formed in this reaction. It is considered that the silyl species **a**, which is prepared via reductive elimination of  $\text{R}_3\text{SiH}$  from **21** in situ, is the active species within the catalytic cycle. Therefore, the generation of a bis(silyl)hydride species is the dormant step. We are currently studying the details of the reaction mechanism.



**Scheme 52** Fe-catalyzed Si–O–Si bond formation reaction from hydrosilane and DMF

Isomerization reactions of allylic alcohols **a** to ketones **b** are catalyzed by various metal (e.g., Ru, Rh, Co, Ni, Mo, Ir, Pt) (Scheme 53) [168–172]. However, these metals are expensive and in some cases harsh reaction conditions are required.

**Scheme 53** Transition metal catalyzed isomerization of allylic alcohols

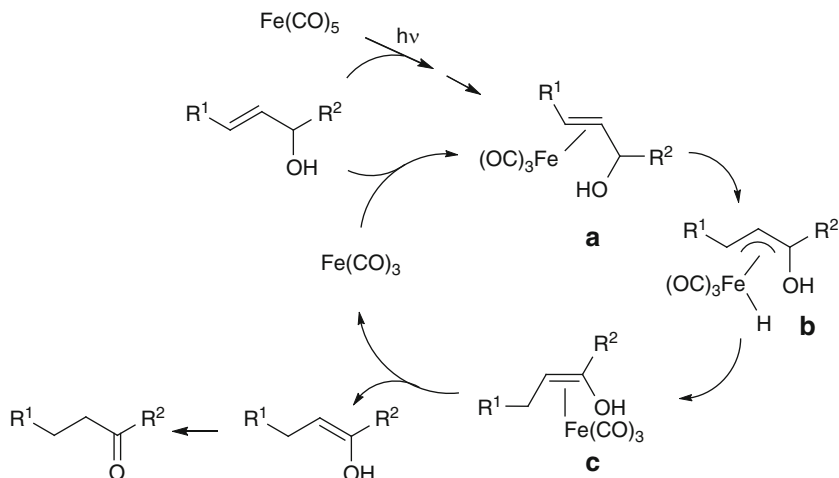


A mild,  $\text{Fe(CO)}_5$ -catalyzed isomerization of this type was reported by Grée and coworkers [173]. Allylic alcohols having mono-, di-, trisubstituted alkene are readily converted into their corresponding ketones, whereas polyunsaturated derivatives do not rearrange (Scheme 54).

The isomerization mechanism is clearly established by labeling experiments. The rearrangement of **a** to **c** via a  $\pi$ -allyl hydride complex **b** in the coordination sphere of the metal is a key step in this catalytic cycle (Scheme 54) [174, 175]. In case of polyunsaturated derivatives, formation of a stable  $\eta^4$  complexes (Scheme 55) is preferred over the rearrangement (**a**  $\rightarrow$  **c**).

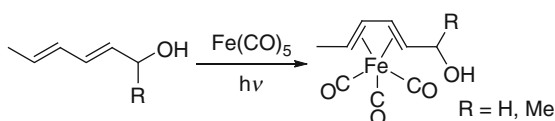
In addition, a 532 (visible) or 355 (UV region) nm laser-induced photoisomerization of allylic alcohols to aldehydes catalyzed by  $[\text{Fe}_3(\text{CO})_{12}]$  or  $[\text{Fe}(\text{CO})_4\text{PPh}_3]$  was developed by Fan [176]. In this reaction, key intermediates such as the  $\pi$ -allyl hydride species  $[\text{FeH}(\text{CO})_3(\eta^3\text{-C}_3\text{H}_3\text{ROH})]$  ( $\text{R} = \text{H}, \text{Me}$ ) were detected by pulsed laser FTIR absorption spectroscopy. These results strongly support the  $\pi$ -allyl mechanism of photoisomerization of allyl alcohols.

Furthermore, details of the isomerization of 1-alkenes into 2-alkenes were examined by deuteration experiments [177] and by using time-resolved IR spectroscopy in

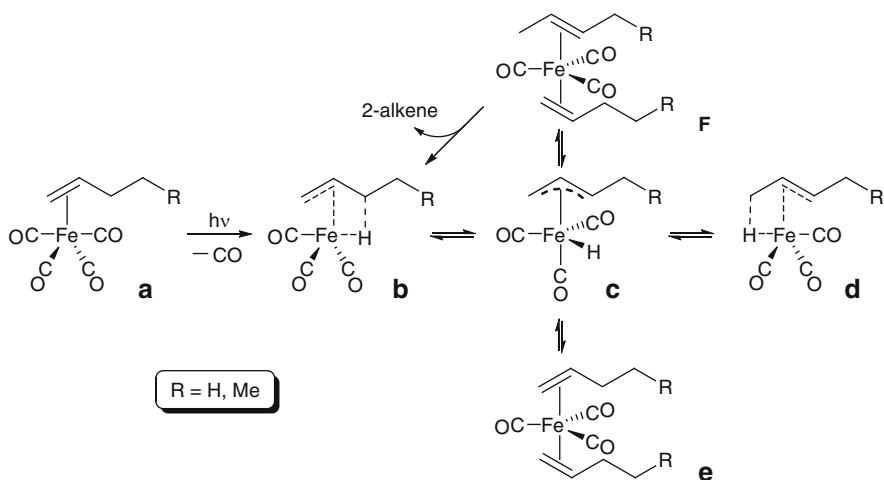


**Scheme 54** Isomerization mechanism of allylic alcohols to ketones

**Scheme 55** Photoreactions of  $\text{Fe}(\text{CO})_5$  with  $\alpha,\beta$ -unsaturated dienol



the gas phase [178] and in solution [179, 180]. The reaction mechanism, which is supported by the DFT calculations, is shown in Scheme 56. Thus, reaction of  $\text{Fe}(\text{CO})_5$  with a 1-alkene under photo-irradiation gives the  $\eta^2$ -alkene complex **a**.



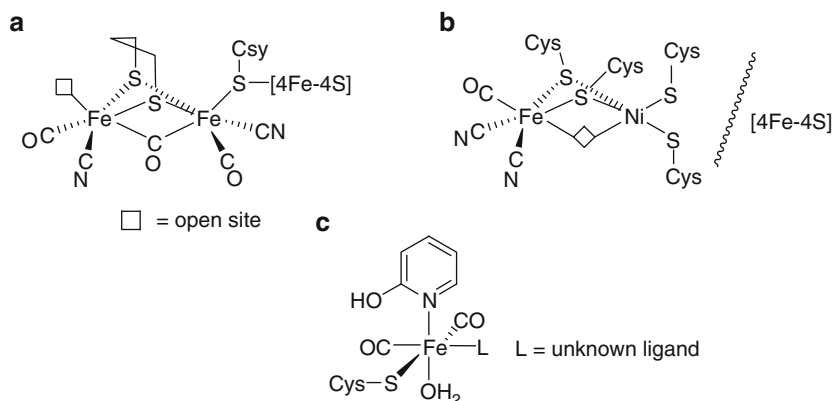
**Scheme 56** Isomerization reaction of 1-alkene catalyzed by an iron complex

Complex **a** is readily converted into a Fe- $\gamma$ -H agnostic complex **b** within an early picosecond timescale and then the  $\pi$ -allyl hydride complex **c** is generated by hydride abstraction. The energy level of the 2-alkene isomer **d**, which is calculated by DFT experiments, is similar to that of the 1-alkene complex **b**. In the next step, Fe(CO)<sub>3</sub>( $\eta^2$ -1-alkene)( $\eta^2$ -2-alkene) **f**, which is generated via intramolecular isomerization of the coordinated 1-alkene to 2-alkene and the coordination of another 1-alkene, is a thermodynamically favored product rather than formation of a Fe(CO)<sub>3</sub>( $\eta^2$ -1-alkene)<sub>2</sub> **e**. Subsequently, release of the 2-alkene from **f** regenerates the active species **b** to complete the catalytic cycle.

## 5 Hydrogen Generation

H<sub>2</sub> serves as the alternative energy source relative to fossil fuels and biomass [181] because it is clean and environmentally friendly. Hence, catalytic hydrogen generation from water under mild conditions is one of the goals for the organometallic catalysis. One of the hopeful methods is the electrochemical reduction of protons by a hydrogenase mimic.

Based upon structural investigations by experts in the field of molecular biology, several Fe-containing complexes are found in the active side of natural proteins, e.g., a diiron complex in [FeFe]-hydrogenases (structure **a** in Fig. 6), a binuclear Fe-Ni complex in [NiFe]-hydrogenases (structure **b** in Fig. 6), or a monoiron complex in [Fe]-hydrogenases (structure **c** in Fig. 6). In [FeFe]-hydrogenases, two Fe centers are bridged by a CO ligand and a small organic moiety. However, it is not clear whether the moiety is a dithiolate ligand or not [182–187]. On the other hand, [NiFe]-hydrogenase is mainly constructed from both a large subunit containing the Ni-Fe cluster [188–190] and a small subunit, an iron-sulfur cluster ([4Fe-4S]). The waved



**Fig. 6** The models for the active site of [FeFe]-, [NiFe]-, and [Fe]-hydrogenases

line stands for the interface between the hydrogenase large subunit and the small subunit [191–193]. The crystal structure of the model for the active site of the [Fe]-hydrogenases is not entirely clear [194, 195].

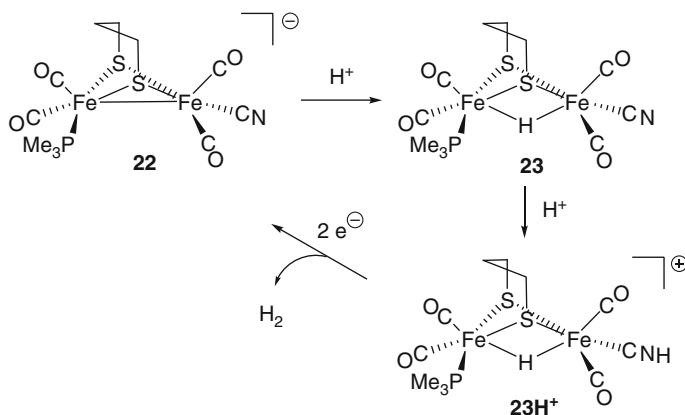
## 5.1 Electrochemical Reduction

Within the past 10 years, various biomimetic Fe model complexes were prepared and their catalytic activities in the electrochemical reduction of protons to H<sub>2</sub> were investigated (Scheme 57).

**Scheme 57** Fe-catalyzed electrochemical reduction of protons to H<sub>2</sub>

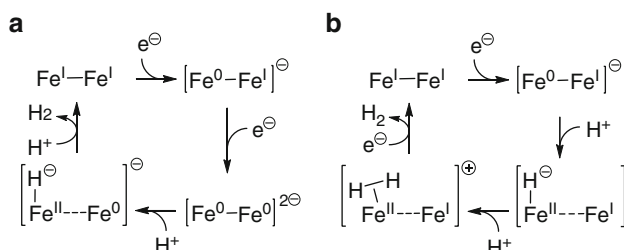


In 2001, Rauchfuss found that the dithiolate diiron complex  $\text{Et}_4\text{N}[\text{Fe}_2\{\mu\text{-S}_2(\text{CH}_2)_3\}(\text{CN})(\text{CO})_4(\text{PMe}_3)_3]$  **22** acts as a catalyst in this reaction under strong acid conditions such as H<sub>2</sub>SO<sub>4</sub>, HCl, and HOTs [196]. In a preparative-scale reaction, a solution of 10<sup>−3</sup> M of **22** with 50 equiv. H<sub>2</sub>SO<sub>4</sub> in CH<sub>3</sub>CN was electrolyzed at −1.2 V. Gas chromatographic analysis showed that the yield of produced H<sub>2</sub> was 100 (±10)%. The proposed catalytic cycle is shown in Scheme 58. Initially, **22** is converted into the μ-hydride complex **23** by metal protonation. A subsequent second protonation at the N atom of the CN<sup>−</sup> ligand affords **23H<sup>+</sup>**. Two-electron reduction of **23H<sup>+</sup>** yields H<sub>2</sub> and regenerates **22**. In this cycle, the μ-hydride complex **23** was isolated by a stoichiometric reaction of **22** with H<sub>2</sub>SO<sub>4</sub> [196] and its structure was confirmed by the X-ray analysis [197].



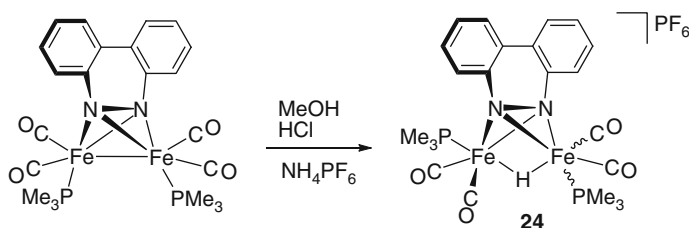
**Scheme 58** Proposed mechanism of the reduction of protons to H<sub>2</sub> catalyzed by **22**

Further investigations of the related dithiolate diiron complexes  $[\text{Fe}_2\{\mu\text{-S}_2(\text{CH}_2)_3\}(\text{CO})_4(\text{L})_2]$  ( $\text{L} = \text{CO}$  or phosphine) were conducted by Rauchfuss's group and Darensbourg's group [197–199] and revealed the catalytic activities to be strongly dependant on the nature of the ligand  $\text{L}$ . Two proposed mechanisms for these complexes are shown in Fig. 7. EECC mechanism (Fig. 7a) is adopted when  $\text{L}$  is a CO ligand, whereas ECCE mechanism (Fig. 7b) is likely for the phosphine complex.



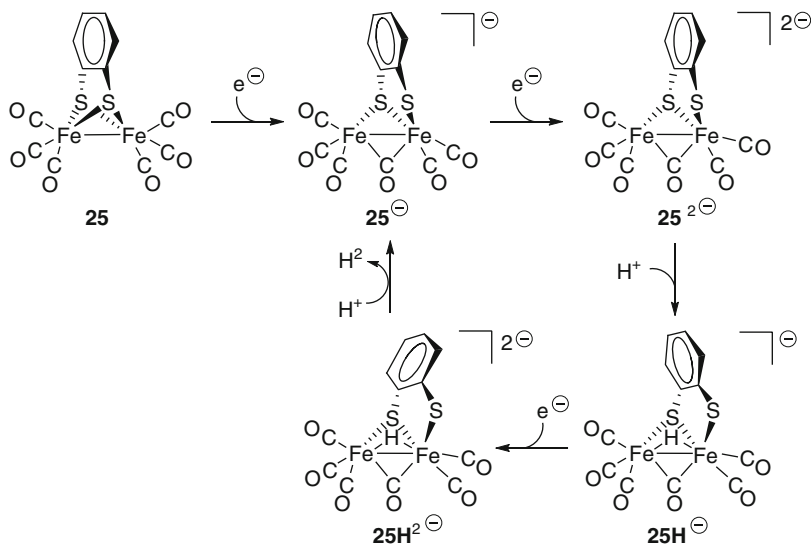
**Fig. 7** Two proposed mechanisms for  $\text{H}_2$  production from  $[\text{Fe}_2\{\mu\text{-S}_2(\text{CH}_2)_3\}(\text{CO})_4(\text{L})_2]$

The  $\mu$ -hydride diiron complex  $[(\mu\text{-H})\text{Fe}_2(\text{BC})(\text{CO})_4(\text{PMe}_3)_2]\text{PF}_6$  **24** ( $\text{BC} = \text{benzo-}[c]\text{-cinnoline}$ ), which was prepared by protonation of  $[\text{Fe}_2(\text{BC})(\text{CO})_4(\text{PMe}_3)_2]$  as a model for the active site of the  $[\text{FeFe}]$ -hydrogenase, was reported by Rauchfuss in 2007 (Scheme 59) [200]. The structure of **24** was confirmed by the X-ray analysis. The electrochemical reduction of protons was attained by using **24** as a catalyst in the presence of *p*-toluenesulfonic acid ( $\text{p}K_{\text{a}} = 8.73$ ).



**Scheme 59** Protonation reaction of  $[\text{Fe}_2(\text{BC})(\text{CO})_4(\text{PMe}_3)_2]$  to form **24**

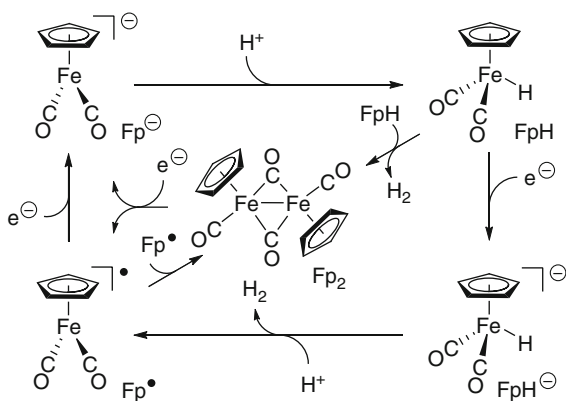
In the same year, Evans and coworkers reported the electrochemical reduction of protons to  $\text{H}_2$  catalyzed by the sulfur-bridged dinuclear iron complex **25** as a hydrogenase mimic in which acetic acid was used as a proton source [201]. The proposed mechanism for this reaction is shown in Scheme 60. The reduction of **25** readily affords  $\text{25}^{2-}$  via a one electron reduction product  $\text{25}^\bullet$ . Protonation of  $\text{25}^{2-}$  by acetic acid produces the  $\mu$ -hydride complex  $\text{25H}^-$  which is reduced to  $\text{25H}^{2-}$ . The obtained  $\text{25H}^{2-}$  reacts with acetic acid to generate molecular hydrogen



**Scheme 60** Proposed mechanism of the reduction of protons to  $H_2$  catalyzed by **25**

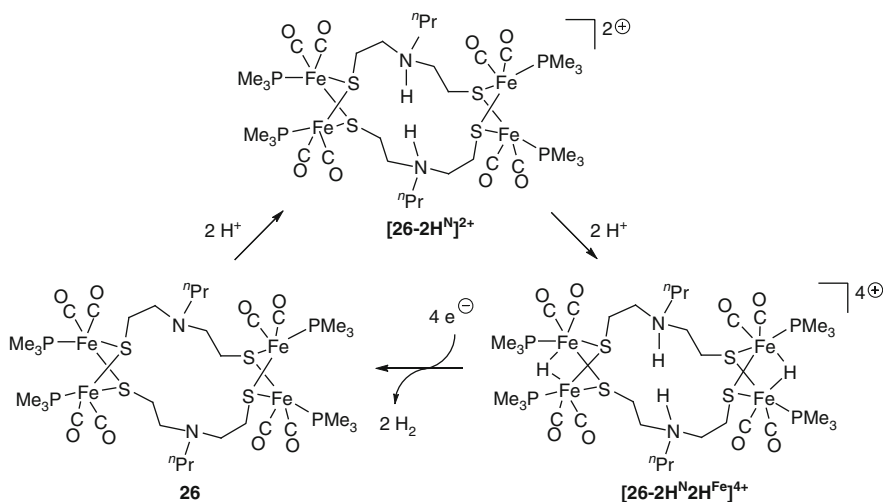
and  $25^-$  to complete the catalytic cycle. This ECEC mechanism was confirmed by calculations and electrochemical experiments.

Evans found that molecular hydrogen was efficiently generated by the reaction of a simple diiron complex  $[CpFe(CO)_2]_2$  ( $Fp_2$ ) with acetic acid ( $pK_a = 22.3$ ) in acetonitrile [202]. Electrochemical simulations revealed that  $Fp_2$ ,  $[CpFe(CO)_2]^-$  ( $Fp^-$ ), and  $[CpFe(CO)_2H]$  ( $FpH$ ) were key intermediates in this catalytic mechanism (Scheme 61). Reduction of  $Fp_2$  produces both an  $Fp^-$  anion and an  $Fp^\bullet$  radical, which is further reduced to give an  $Fp^-$  anion. The oxidation of the  $Fp^-$  anion by proton affords  $FpH$ . This protonation was found to be the rate-limiting step. The dimerization of the  $FpH$  generates  $Fp_2$  and  $H_2$ . Alternatively, the  $FpH$  is reduced to afford the  $FpH^-$  anion, which is subsequently protonated



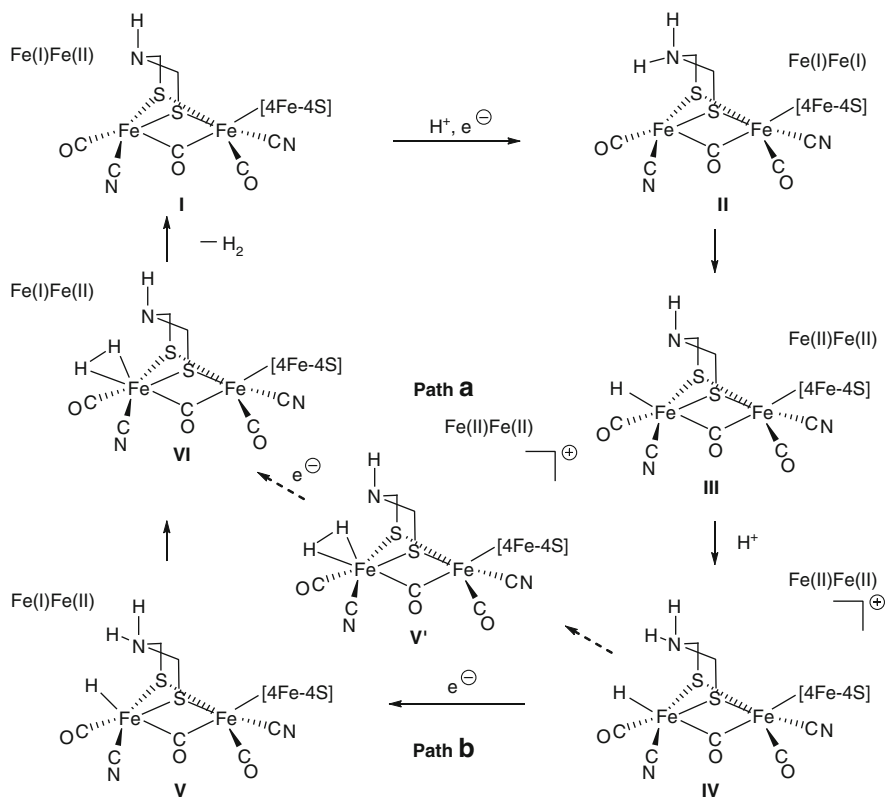
**Scheme 61**  $[CpFe(CO)_2]_2$  reduction followed by catalytic reduction of protons to  $H_2$

Chiang and coworkers synthesized a dimer of compound **26** in which two diiron subunits are linked by two azadithiolate ligands as a model of the active site for the [FeFe]-hydrogenase [203]. Protonation of **26** afforded the  $\mu$ -hydride complex  $[\mathbf{26}\text{-}2\text{H}^{\text{N}}2\text{H}^{\text{Fe}}]^{4+}$  via the initially protonated species  $[\mathbf{26}\text{-}2\text{H}^{\text{N}}]^{2+}$  (Scheme 62). These three complexes were also characterized by the X-ray diffraction analyses.  $\text{H}_2$ -generation was observed by electrochemical reduction of protons catalyzed by **26** in the presence of  $\text{HBF}_4$  as a proton source. It was experimentally ascertained that  $[\mathbf{26}\text{-}2\text{H}^{\text{N}}2\text{H}^{\text{Fe}}]^{4+}$  was converted into **26** by four irreversible reduction steps in the absence of  $\text{HBF}_4$ .



**Scheme 62** Reaction scheme of dimer of dimer iron complexes as models

The proposed mechanism of H<sub>2</sub> evolution by a model of [FeFe]-hydrogenases based upon DFT calculations [204–206] and a hybrid quantum mechanical and molecular mechanical (QM/MM) investigation is summarized in Scheme 63 [207]. Complex **I** is converted into **II** by both protonation and reduction. Migration of the proton on the N atom to the Fe center in **II** produces the hydride complex **III**, and then protonation affords **IV**. In the next step, two pathways are conceivable. One is that the molecular hydrogen complex **VI** is synthesized by proton transfer and subsequent reduction (Path **a**). The other proposed by De Gioia, Ryde, and coworkers [207] is that the reduction of **IV** affords **VI** via the terminal hydride complex **V** (Path **b**). Dehydrogenation from **VI** regenerates **I**.

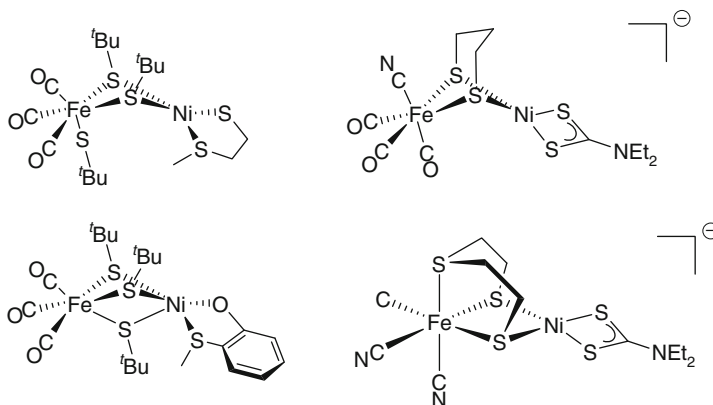


**Scheme 63** Two pathways for catalytic mechanism of the Enzymatic  $H_2$  production

Although the mechanistic insights for the model complex of [FeFe] hydrogenase became clearer little by little, those for the [NiFe] hydrogenase are still challenging topics.

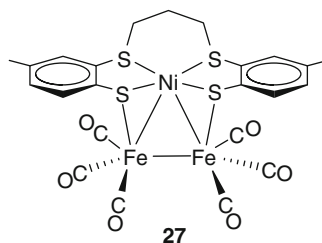
Heterodinuclear Ni–Fe complexes, which are not stabilized by the phosphine and NO ligands, were synthesized by Tatsumi and coworkers as [NiFe] hydrogenase mimics [208–210]. Several examples are shown in Fig. 8. However, the catalytic activities of these complexes are not ascertained.

The first electrochemical  $H_2$  generation catalyzed by a hetero-nuclear Fe–Ni complex  $[Ni(L)Fe_2(CO)_6]$  (**27**)  $[L^{2-} = (CH_3C_6H_3S_2)_2(CH_2)_3^{2-}]$  (Fig. 9) with trifluoroacetic acid was reported by Schöder and coworkers in 2006 [211]. Based on their electrochemical behavior, spectroscopic data, and DFT calculations of **27**, an EECC mechanism was ruled out and therefore an ECCE or ECEC mechanism involving the formation of  $Fe^{II}-H^-$  and  $Ni^{III}-H^-$  intermediates is likely. In this cycle, six catalytic turnovers were achieved. This value is comparable to those for  $[Fe_2(X)(CO)_4(PMe_3)_2]$   $[X = 2(EtS^-), pdt^{2-}, edt^{2-}, xyldt^{2-}]$  (ca. 6–30 TON) [198, 199].

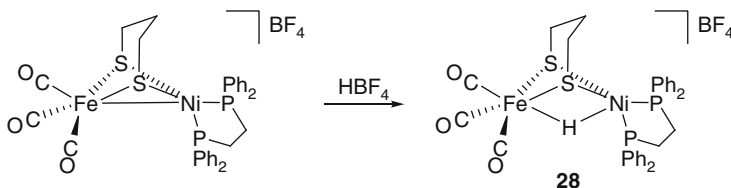


**Fig. 8** The model complexes for [NiFe]-hydrogenases

**Fig. 9** Electrochemical  $\text{H}_2$  generation catalyzed by complex **27** as a model for the [NiFe] hydrogenase

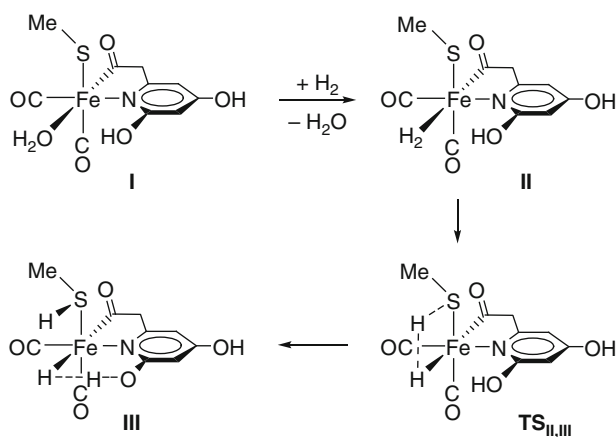


In 2009, Rauchfuss and coworkers succeeded in the synthesis of the Fe- $\mu$ -H-Ni complex  $[(\text{CO})_3\text{Fe}(\text{pdt})(\mu\text{-H})\text{Ni}(\text{dppe})]\text{BF}_4$  **28** (pdt = 1,3-propanedithiolate, dppe = 1,2- $\text{C}_2\text{H}_4(\text{PPh}_2)_2$ ) as a model for [NiFe]-hydrogenases (Scheme 64) [212]. The structure of **28** was characterized by X-ray crystallographic analysis. This is the first example of an Fe-Ni thiolato hydride complex. Evolution of  $\text{H}_2$  by electrochemical reduction of  $\text{CF}_3\text{CO}_2\text{H}$  ( $\text{p}K_{\text{a}} = 12.65$ ) was observed in the presence of the catalytic amounts of **28**.



**Scheme 64** Protonation reaction of  $(\text{CO})_3\text{Fe}(\text{pdt})\text{Ni}(\text{dppe})$  to form **28**

Yang and Hall investigated mechanistic details for the H–H bond cleavage by mononuclear [Fe]-hydrogenases using computational methods (Scheme 65) [213]. Accordingly, model complex **I** reacts with  $\text{H}_2$  to give the dihydrogen complex **II**, which is subsequently converted into the hydride complex **III** via **TS<sub>II,III</sub>** for the cleavage of  $\text{H}_2$  with sulfur as a proton acceptor. Complex **III** shows strong interaction through  $\text{Fe}-\text{H}^{\delta-} \cdots \text{H}^{\delta+}-\text{O}$  dihydrogen bond.

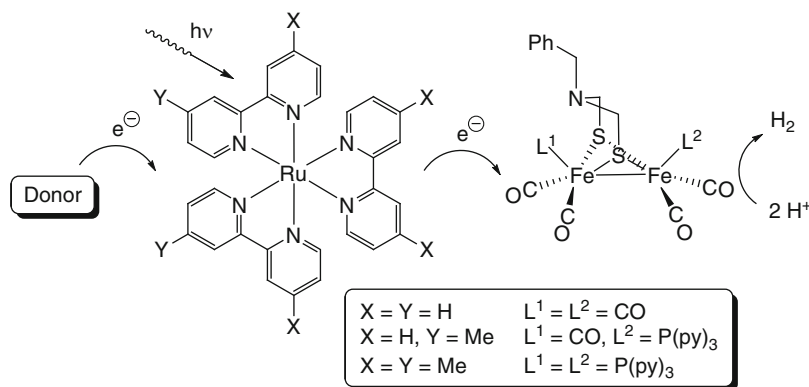


**Scheme 65** The calculated mechanism of H–H bond cleavage reaction of the model complex for [Fe]-hydrogenases

## 5.2 Photochemical Reduction

Transition-metal catalyzed photochemical reactions for hydrogen generation from water have recently been investigated in detail. The reaction system is composed of three major components such as a photosensitizer (PS), a water reduction catalyst (WRC), and a sacrificial reagent (SR). Although noble-metal complexes as WRC have been used [214–230], examples for iron complexes are quite rare. It is well known that a hydride as well as a dihydrogen (or dihydride) complex plays important roles in this reaction.

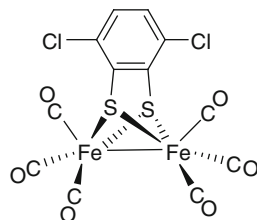
An iron-catalyzed photochemical hydrogen generation from water was developed by Wang, Sun, and coworkers in 2008 [231]. A three component catalyst system (a ruthenium polypyridine derivative as the PS, a dithiolate diiron complex as the WRC, ascorbic acid as both electron and proton donor (SR)) in  $\text{CH}_3\text{CN}/\text{H}_2\text{O}$  under photo-irradiation conditions showed catalytic activity in the hydrogen generation (Scheme 66). Although the visible light-driven hydrogen generation from water proved successful, the catalytic activity is not high (up to 4.3 TON based on the iron complex).



**Scheme 66** Photochemical hydrogen generation catalyzed by the model complex of [FeFe]-hydrogenases

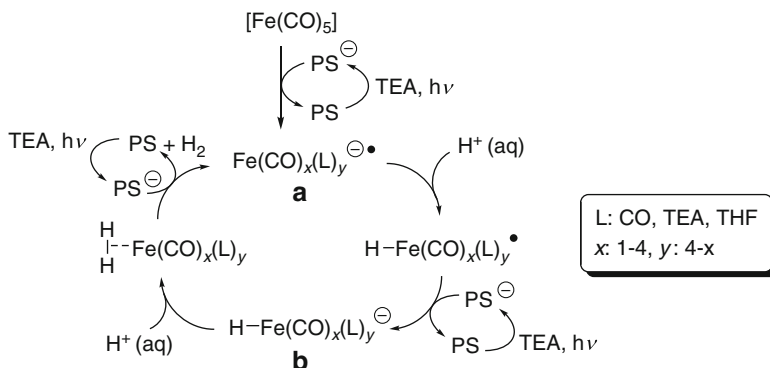
Very recently, Hammarström, Ott, and coworkers found that the catalytic activity was significantly increased (up to 200 TON based on the iron complex) when a diiron complex having a 3,6-dichlorobenzene-1,2-dithiolate ligand (Fig. 10) instead of a benzylazadithiolate ligand was used as a WRC (see ref. [64] in [232]).

**Fig. 10** Diiron complex having a 3,6-dichlorobenzene-1,2-dithiolate ligand as a catalyst for the hydrogen generation



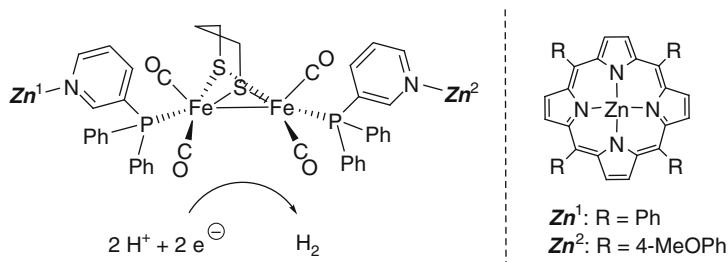
Recently, Beller and coworkers reported another efficient Fe-catalyzed light-driven hydrogen generation system [233]. The highest activity for the iron complex was achieved by using the combination of  $[\text{Ir}(\text{bpy})(\text{ppy})_2][\text{PF}_6]$  as the PS, an iron(0) carbonyl complex as the WRC, and triethylamine (TEA) as the SR under photolysis conditions. The maximum TON was 322 based on the iron complex. The mechanism for the photochemical reduction of water, which is similar to the one proposed by Wang, Sun, and coworkers [231], is shown in Scheme 67. The iron carbonyl species **a** is generated by reduction of  $[\text{Fe}(\text{CO})_5]$  by the  $\text{PS}^-$ , which is generated by photoreaction of PS and TEA as the SR. Protonation and reduction of **a** affords the hydride species **b**, which is subsequently protonated to give dihydrogen with regeneration of **a**.

Two different types of zinc-porphyrins coordinated diiron complex act as catalysts for the photochemical reduction hydrogen evolution from water. In this system



**Scheme 67** The proposed mechanism for iron-catalyzed light-driven hydrogen generation from water

achieved by Hartl and coworkers (Scheme 68) [234], two different chromophores ( $\text{Zn}^1$  and  $\text{Zn}^2$ ) and a tertiary amine  $\text{N}^i\text{Pr}_2\text{Et}$  as a SR for the electron donor are required.



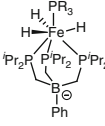
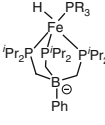
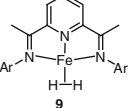
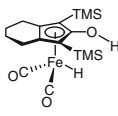
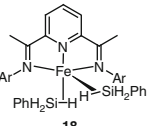
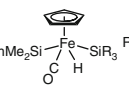
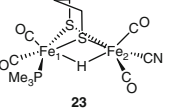
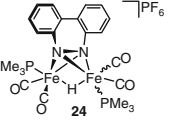
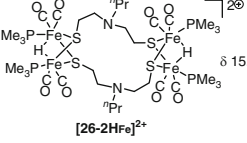
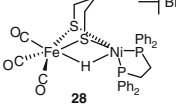
**Scheme 68** The molecular hydrogen evolution catalyzed by self-assembled Zn–Fe–Zn complex

**Acknowledgment** We would like to show our respect for the great efforts of all authors, whose names were listed in the references. We wish to thank Dr. Yuji Suzuki for the reference collection.

## Appendix

The isolated iron hydride complexes introduced in this chapter are listed in Table 12, where the hydride chemical shifts in the  $^1\text{H}$ NMR spectra and the Fe–H bond distances are summarized.

Table 12

Complex	$^1\text{H}$ NMR hydride signal ( $\delta$ , ppm)	X-ray analysis Fe-H bond distance ( $\text{\AA}$ )	Ref.
 <p><math>\text{R}_3 = \text{Me}_3</math>: <b>3</b>  <math>\text{Et}_3</math>: <b>4</b>  <math>\text{MePh}_2</math></p>	$\delta$ 13.72 (s) <sup>a</sup> $\delta$ 13.16 (s) <sup>a</sup> $\delta$ 13.16 (s) <sup>a</sup>	1.44(2), 1.46(3), 1.51(2)	[26] [26] [26]
 <p><math>\text{R}_3 = \text{Me}_3</math>  <math>\text{MePh}_2</math></p>	$\delta$ 2.34 (br, s) N.D.	1.511(14) 1.363(13)	[26] [26]
 <p><b>9</b></p>	N.D.		[27]
 <p><b>11</b></p>	$\delta$ 11.62 (s)	1.38(2)	[235] [47] (for catalytic reaction)
 <p><b>18</b></p>	$\delta$ 6.69 (s)	1.45(3), 1.51(3)	[27]
 <p><math>\text{PhMe}_2\text{Si}</math> <math>\text{Fe}</math> <math>\text{SiR}_3</math> <math>\text{R}_3 = \text{Me}_2\text{Ph}</math>: <b>21</b>  <math>\text{Et}</math></p>	$\delta$ 13.22 (s) $\delta$ 13.71 (s)	1.44(3) 1.46(3)	[166,167]
 <p><b>23</b></p>	$\delta$ 17.08 (d, $J_{\text{PH}} = 24$ Hz)	1.70(2) for $\text{Fe}_1$ 1.63(2) for $\text{Fe}_2$	[197]
 <p><b>24</b></p>	$\delta$ 15.479 (dd, $J_{\text{PH}} = 8, 26.5$ Hz, <i>unsym</i> ) $\delta$ 15.621 (dd, $J_{\text{PH}} = 9$ Hz, <i>sym</i> )	1.62(3) for <i>sym</i>	[200] [200]
 <p><b>[26-2HFe]<math>^{2+}</math></b></p>	$\delta$ 15.46 (d, $J_{\text{PH}} = 21.5$ Hz)	1.620 <sup>b</sup> , 1.668 <sup>b</sup>	[203]
 <p><b>28</b></p>	$\delta$ 3.53 (tt, $J_{\text{PH}} = 6$ Hz, $J_{\text{HH}} = 0.6$ Hz)	1.46(6)	[212]

<sup>a</sup> $^1\text{H}\{^{31}\text{P}\}$  NMR measurement.

<sup>b</sup>The bond distances were calculated by Mercury 2.2 for Windows [236] using CIF data.

## References

1. Connelly NG, Damhus T, Hartshorn RM, Hutton AT (eds) (2005) Nomenclature of Inorganic Chemistry IUPAC Recommendations 2005
2. Hieber W, Leutert F (1931) *Naturwissenschaften* 19:360
3. Weichselfelder T, Thiede B (1926) *Justus Liebigs Ann Chem* 447:64
4. Dahl LF, Blount JF (1965) *Inorg Chem* 4:1373
5. Manojlović-Muir L, Muir KW, Ibers JA (1970) *Inorg Chem* 9:447
6. Guggenberger LJ, Titus DD, Flood MT, Marsh RE, Orto AA, Gray HB (1972) *J Am Chem Soc* 94:1135
7. Esteruelas MA, Oro LA (1998) *Chem Rev* 98:577
8. Morris RH, Sawyer JF, Shiralian M, Zubkowski JD (1985) *J Am Chem Soc* 107:5581
9. Bianchini C, Peruzzini M, Zanolini F (1988) *J Organomet Chem* 354:C19
10. Field LD, Messerle BA, Smernik RJ (1997) *Inorg Chem* 36:5984
11. Stoppioni P, Mani F, Sacconi L (1974) *Inorg Chim Acta* 11:227
12. Plietker B (ed) (2008) *Iron catalysis in organic chemistry*, Wiley-VCH, Weinheim
13. Bolm C, Legros J, Le Pailh J, Zani L (2004) *Chem Rev* 104:6217
14. Fürstner A, Martin R (2005) *Chem Lett* 34:624
15. Correa A, Mancheño OG, Bolm C (2008) *Chem Soc Rev* 37:1108
16. Sherry BD, Fürstner A (2008) *Acc Chem Res* 41:1500
17. Gaillard S, Renaud J-L (2008) *ChemSusChem* 1:505
18. Enthaler S, Junge K, Beller M (2008) *Angew Chem* 120:3363, *Angew Chem Int Ed* 47:3317
19. Sarhan AAO, Bolm C (2009) *Chem Soc Rev* 38:2730
20. Chen MS, White MC (2007) *Science* 318:783
21. Frankel EN, Emken EA, Peters HM, Davison VL, Butterfield RO (1964) *J Org Chem* 29:3292
22. Frankel EN, Emken EA, Davison VL (1965) *J Org Chem* 30:2739
23. Harmon RE, Gupta SK, Brown DJ (1973) *Chem Rev* 73:21
24. Schroder MA, Wrighton MS (1976) *J Am Chem Soc* 98:551
25. Kismartoni LC, Weitz E, Cedeno DL (2005) *Organometallics* 24:4714
26. Daida EJ, Peters JC (2004) *Inorg Chem* 43:7474
27. Bart SC, Lobkovsky E, Chirik PJ (2004) *J Am Chem Soc* 126:13794
28. Bart SC, Chlopek K, Bill E, Bouwkamp MW, Lobkovsky E, Neese F, Wieghardt K, Chirik PJ (2006) *J Am Chem Soc* 128:13901
29. Bart SC, Hawrelak EJ, Lobkovsky E, Chirik PJ (2005) *Organometallics* 24:5518
30. Trovitch RJ, Lobkovsky E, Bill E, Chirik PJ (2008) *Organometallics* 27:1470
31. Archer AM, Bouwkamp MW, Cortez M-P, Lobkovsky E, Chirik PJ (2006) *Organometallics* 25:4269
32. Noyori R, Ohkuma T (2001) *Angew Chem Int Ed* 40:40
33. Ikariya T, Murata K, Noyori R (2006) *Org Biomol Chem* 4:393
34. Shvo Y, Czarkie D, Rahamim Y, Chodosh DF (1986) *J Am Chem Soc* 108:7400
35. Casey CP, Singer SW, Powell DR, Hayashi RK, Kavana M (2001) *J Am Chem Soc* 123:1090
36. Santosh Laxmi YR, Bäckvall J-E (2000) *Chem Commun* 611
37. Lau CP, Ng SM, Jia G, Lin Z (2007) *Coord Chem Rev* 251:2223
38. Noyori R, Kitamura M, Ohkuma T (2004) *Proc Natl Acad Sci USA* 101:5356
39. Clapham SE, Hadzovic A, Morris RH (2004) *Coord Chem Rev* 248:2201
40. Conley BL, Pennington-Boggio MK, Boz E, Williams TJ (2010) *Chem Rev* 110:2294
41. Blum Y, Czarkie D, Rahamim Y, Shvo Y (1985) *Organometallics* 4:1459
42. Shvo Y, Czarkie D, Rahamim Y, Chodosh DF (1986) *J Am Chem Soc* 108:7400
43. Menashe N, Shvo Y (1991) *Organometallics* 10:3885
44. Menashe N, Salant E, Shvo Y (1996) *J Organomet Chem* 514:97
45. Noyori R, Ohkuma T (1999) *Pure Appl Chem* 71:1493

46. Doucet H, Ohkuma T, Murata K, Yokozama T, Kozawa M, Katayama E, England AF, Ikariya T, Noyori R (1998) *Angew Chem Int Ed* 37:1703
47. Casey CP, Guan H (2007) *J Am Chem Soc* 129:5816
48. Casey CP, Guan H (2009) *J Am Chem Soc* 131:2499
49. Sui-Seng C, Freutel F, Lough AJ, Morris RH (2008) *Angew Chem Int Ed* 47:940
50. Hashiguchi S, Fujii A, Takehara J, Ikariya T, Noyori R (1995) *J Am Chem Soc* 117:7562
51. Rautenstrauch V, Hoang-Cong X, Churlaud R, Abdur-Rashid K, Morris RH (2003) *Chem Eur J* 9:4954
52. Mikhailine A, Lough AJ, Morris RH (2009) *J Am Chem Soc* 131:1394
53. Enthaler S, Erre G, Tse MK, Junge K, Beller M (2006) *Tetrahedron Lett* 47:8095
54. Enthaler S, Hagemann B, Erre G, Junge K, Beller M (2006) *Chem Asian J* 1:598
55. Zassinovich G, Mestroni G, Gladiali S (1992) *Chem Rev* 92:1051
56. Gladiali S, Mestroni G (2004) In: Beller M, Bolm C (eds) *Transition metals for organic synthesis*, 2nd edn. Wiley-VCH, Weinheim, p 145
57. Gladiali S, Alberico E (2006) *Chem Soc Rev* 35:226
58. Thorson MK, Klinkel KL, Wang J, Williams TJ (2009) *Eur J Inorg Chem* 295
59. Ojima I (1989) In: Patai S, Rapoport Z (eds) *The chemistry of organosilicon compounds*, Wiley, New York
60. Brook MA (2000) *Silicon in organic, organometallic, and polymer chemistry*. Wiley, New York
61. Marciniak B (ed) (1992) *Comprehensive handbook on hydrosilylation*. Pergamon, Oxford
62. Marciniak B (1996) In: Cornils B, Herrmann WA (eds) *Applied homogeneous catalysis with organometallic compounds*, vol 1. Weinheim, Wiley-VCH, Chap 2
63. Speier JL (1979) *Adv Organomet Chem* 17:407
64. Marciniak B, Guliński J (1993) *J Organomet Chem* 446:15
65. Nishiyama H, Furuta A (2007) *Chem Commun* 760
66. Furuta A, Nishiyama H (2008) *Tetrahedron Lett* 49:110
67. Shaikh NS, Junge K, Beller M (2007) *Org Lett* 9:5429
68. Shaikh NS, Enthaler S, Junge K, Beller M (2008) *Angew Chem Int Ed* 47:2497
69. Nishibayashi Y, Takei I, Uemura S, Hidaï M (1998) *Organometallics* 17:3420
70. Yun J, Buchwald SL (1999) *J Am Chem Soc* 121:5640
71. Langlotz BK, Wadepohl H, Gade LH (2008) *Angew Chem Int Ed* 47:4670
72. Tondreau AM, Lobkovsky E, Chirik PJ (2008) *Org Lett* 10:2789
73. Tondreau AM, Darmon JM, Wile BM, Floyd SK, Lobkovsky E, Chirik PJ (2009) *Organometallics* 28:3928
74. Brown HC, Zaidlewicz M (2001) In: *Organic Syntheses via Boranes*, Vol 2. Aldrich Chemical Company, Milwaukee, p 118
75. Yamamoto Y, Asao N (1993) *Chem Rev* 93:2207
76. Bubnov YN (1987) *Pure Appl Chem* 59:895
77. Brown HC, Zaidlewicz M (2001) *Organic syntheses via boranes*, Vol 2. Aldrich Chemical Company, Milwaukee, WI, pp 189 and 207
78. Kennedy JWJ, Hall DG (2003) *Angew Chem Int Ed* 42:4732
79. Sugiura M, Hirano K, Kobayashi S (2004) *J Am Chem Soc* 126:7182
80. Solin N, Wallner OA, Szabó KJ (2005) *Org Lett* 7:689
81. Lou S, Moquist PN, Schaus SE (2007) *J Am Chem Soc* 129:15398
82. Sebelius S, Olsson VJ, Wallner OA, Szabó KJ (2006) *J Am Chem Soc* 128:8150
83. Burgess K, Ohlmeyer MJ (1991) *Chem Rev* 91:1179
84. Beletskaya I, Pelter A (1997) *Tetrahedron* 53:4957
85. Satoh M, Nomoto Y, Miyaura N, Suzuki A (1989) *Tetrahedron Lett* 30:3789
86. Zaidlewicz M, Meller J (1997) *Tetrahedron Lett* 38:7279
87. Matsumoto Y, Hayashi T (1991) *Tetrahedron Lett* 32:3387
88. Wu JY, Moreau B, Ritter T (2009) *J Am Chem Soc* 131:12915
89. Sugimoto M, Ohmori Y, Ito Y (2000) *J Organomet Chem* 611:403
90. Nakamura M, Matsuo K, Ito S, Nakamura E (2004) *J Am Chem Soc* 126:3686

91. Sapountzis I, Lin W, Kofink CC, Despotopoulou C, Knochel P (2005) *Angew Chem* 117:1682, *Angew Chem Int Ed* 44:1654
92. Plietker B (2006) *Angew Chem* 118:6200, *Angew Chem Int Ed* 45:6053
93. Cahiez G, Habiak V, Duplais C, Moyeux A (2007) *Angew Chem* 119:4442, *Angew Chem Int Ed* 46:4364
94. Guérinot A, Reymond S, Cossy J (2007) *Angew Chem* 119:6641, *Angew Chem Int Ed* 46:6521
95. Fürstner A, Martin R, Krause H, Seidel G, Goddard R, Lehmann CW (2008) *J Am Chem Soc* 130:8773
96. Carril M, Correa A, Bolm C (2008) *Angew Chem* 120:4940, *Angew Chem Int Ed* 47:4862
97. Czaplik WM, Mayer M, Wangelin AJ (2009) *Angew Chem* 121:616, *Angew Chem Int Ed* 48:607
98. Yoshikai N, Matsumoto A, Norinder J, Nakamura E (2009) *Angew Chem* 121:2969, *Angew Chem Int Ed* 48:2925
99. Cahiez G, Foulgoc L, Moyeux A (2009) *Angew Chem* 121:3013, *Angew Chem Int Ed* 48:2969
100. Li Y-Z, Li B-J, Lu X-Y, Lin S, Shi Z-J (2009) *Angew Chem* 121:3875, *Angew Chem Int Ed* 48:3817
101. Li Z, Cao L, Li C-J (2007) *Angew Chem* 119:6625, *Angew Chem Int Ed* 46:6505
102. Li Z, Yu R, Li H (2008) *Angew Chem* 120:7607, *Angew Chem Int Ed* 47:7497
103. Zhang Y, Li C-J (2007) *Eur J Org Chem* 4654
104. Nagano T, Hayashi T (2004) *Org Lett* 6:1297
105. Zhang D, Ready JM (2006) *J Am Chem Soc* 128:15050
106. Duboudin JG, Jousseau B, Bonakdar A, Saux A (1979) *J Organomet Chem* 168:227
107. Lu Z, Ma S (2006) *J Org Chem* 71:2655
108. Moreau B, Wu JY, Ritter T (2009) *Org Lett* 11:337
109. Zhang S-Y, Tu Y-Q, Fan C-A, Zhang F-M, Shi L (2009) *Angew Chem Int Ed* 48:8761
110. Driller KM, Klein H, Jackstell R, Beller M (2009) *Angew Chem Int Ed* 48:6041
111. Periasamy M, Rameshkumar C, Radhakrishnan U (1997) *Tetrahedron Lett* 38:7229
112. Periasamy M, Rameshkumar C, Radhakrishnan U, Brunet J-J (1998) *J Org Chem* 63:4930
113. Rameshkumar C, Periasamy M (2000) *Organometallics* 19:2400
114. Rameshkumar C, Periasamy M (2000) *Tetrahedron Lett* 41:2719
115. Periasamy M, Mukkanti A, Raj DS (2004) *Organometallics* 23:6323
116. Periasamy M, Mukkanti A, Raj DS (2004) *Organometallics* 23:619
117. Rameshkumar C, Periasamy M (2000) *Synlett* 1619
118. Periasamy M, Rameshkumar C, Mukkati A (2002) *J Organomet Chem* 649:209
119. Sylvester KT, Chirik PJ (2009) *J Am Chem Soc* 131:8772
120. Jang H-Y, Krische MJ (2004) *Acc Chem Res* 37:653
121. Small BL, Brookhart M, Bennett AMA (1998) *J Am Chem Soc* 120:4049
122. Small BL, Brookhart M (1998) *J Am Chem Soc* 120:7143
123. Britovsek GJP, Gibson VC, Kimberley BS, Maddox PJ, McTavish SJ, Solan GA, White AJP, Williams DJ (1998) *Chem Commun* 849
124. Britovsek GJP, Bruce M, Gibson VC, Kimberley BS, Maddox PJ, Mastroianni S, McTavish SJ, Redshaw C, Solan GA, Strömberg S, White AJP, Williams DJ (1999) *J Am Chem Soc* 121:8728
125. Britovsek GJP, Mastroianni S, Solan GA, Baugh SPD, Redshaw C, Gibson VC, White AJP, Williams DJ, Elsegood MRJ (2000) *Chem Eur J* 6:2221
126. Small BL, Marcucci AJ (2001) *Organometallics* 20:5738
127. Babik ST, Fink G (2002) *J Mol Cat A: Chem* 188:245
128. Khoroshun DV, Musaev DG, Vreven T, Morokuma K (2001) *Organometallics* 20:2007
129. Raucoules R, de Bruin T, Raybaud P, Adamo C (2009) *Organometallics* 28:5358
130. Kadyrov R, Riermeier TH (2003) *Angew Chem* 115:5630, *Angew Chem Int Ed* 42:5472
131. Bunlaksananusorn T, Rampf F (2005) *Synlett* 2682

132. Hamid MHSA, Williams MJ (2007) *Chem Commun* 725
133. Tararov VI, Börner A (2005) *Synlett* 203
134. Tararov VI, Kadyrov R, Riermeier TH, Fischer C, Börner A (2004) *Adv Synth Catal* 346:561
135. Tararov VI, Kadyrov R, Riermeier TH, Börner A (2002) *Adv Synth Catal* 344:200
136. Tararov VI, Kadyrov R, Riermeier TH, Börner A (2000) *Chem Commun* 1867
137. Kadyrov R, Riermeier TH, Dingerdissen U, Tararov V, Börner A (2003) *J Org Chem* 68:4067
138. Kitamura M, Lee D, Hayashi S, Tanaka S, Yoshimura M (2002) *J Org Chem* 67:8685
139. Imao D, Fujihara S, Yamamoto T, Ohta T, Ito Y (2005) *Tetrahedron* 61:6988
140. Fujita K-I, Yamaguchi R (2005) *Synlett* 560
141. Chi Y, Zhou Y-G, Zhang X (2003) *J Org Chem* 68:4120
142. Blank B, Madalska M, Kempe R (2008) *Adv Synth Catal* 350:749
143. Robichaud A, Nait Ajjou A (2006) *Tetrahedron Lett* 47:3633
144. Bhor MD, Bhanushali MJ, Nandurkar NS, Bhanage BM (2008) *Tetrahedron Lett* 49:965
145. Zhou S, Addis D, Das S, Junge K, Beller M (2009) *Chem Commun* 4883
146. Hanada S, Motoyama Y, Nagashima H (2008) *Eur J Org Chem* 4097
147. Zhou S, Junge K, Addis D, Das S, Beller M (2009) *Angew Chem Int Ed* 48:9507
148. Sunada Y, Kawakami H, Imaoka T, Motoyama Y, Nagashima H (2009) *Angew Chem Int Ed* 48:9511
149. Iwanami K, Seo H, Tobita Y, Oriyama T (2005) *Synthesis* 183
150. Iwanami K, Yano K, Oriyama T (2005) *Synthesis* 2669
151. Iwanami K, Yano K, Oriyama T (2007) *Chem Lett* 36:38
152. Doyle MP, DeBruyn DJ, Kooistra DA (1972) *J Am Chem Soc* 94:3659
153. Nicolaou KC, Hwang C-K, Nugiel DA (1989) *J Am Chem Soc* 111:4136
154. Izumi M, Fukase K (2005) *Chem Lett* 34:594
155. Kato J-I, Iwasawa N, Mukaiyama T (1985) *Chem Lett* 743
156. Sassaman MB, Kotian KD, Prakash GKS, Olah GA (1987) *J Org Chem* 52:4314
157. Hatakeyama S, Mori H, Kitano K, Yamada H, Nishizawa M (1994) *Tetrahedron Lett* 35:4367
158. Komatsu N, Ishida J, Suzuki H (1997) *Tetrahedron Lett* 38:7219
159. Bajwa JS, Jiang X, Slade J, Prasad K, Repič O, Blacklock TJ (2002) *Tetrahedron Lett* 43:6709
160. Yang W-C, Lu X-A, Kulkarni SS, Hung S-C (2003) *Tetrahedron Lett* 44:7837
161. Chandrasekhar S, Chandrashekar G, Babu BN, Vijeender K, Venkatram Reddy K (2004) *Tetrahedron Lett* 45:5497
162. Wada M, Nagayama S, Mizutani K, Hiroi R, Miyoshi N (2002) *Chem Lett* 248
163. Nakazawa H, Kamata K, Itazaki M (2005) *Chem Commun* 4004
164. Nakazawa H, Itazaki M, Kamata K, Ueda K (2007) *Chem Asian J* 2:882
165. Nakazawa H, Kawasaki T, Miyoshi K, Suresh CH, Koga N (2004) *Organometallics* 23:117
166. Itazaki M, Ueda K, Nakazawa H (2009) *Angew Chem Int Ed* 48:3313; *ibid* 48: 6938
167. Sharma HK, Pannell KH (2009) *Angew Chem Int Ed* 48:7052
168. Trost BM, Kulawiec RJ (1993) *J Am Chem Soc* 115:2027 (and references cited therein)
169. Bäckvall JE, Andreasson U (1993) *Tetrahedron Lett* 34:5459
170. Marko IE, Gautier A, Tsukazaki M, Llobet A, Plantalech-Mir E, Urch CJ, Brown SM (1999) *Angew Chem Int Ed* 38:1960
171. Slugovc C, Rüba E, Schmid R, Kirchner K (1999) *Organometallics* 18:4230
172. Ni Bricourt H, Monflier E, Carpentier J-F, Mortreux A (1998) *Eur J Inorg Chem* 1739
173. Cherkaoui H, Soufiaoui M, Grée R (2001) *Tetrahedron* 57:2379
174. Hendrix WT, Cowherd FG, von Rosenberg JL (1968) *Chem Commun* 97
175. Strauss JU, Ford PW (1975) *Tetrahedron Lett* 2917
176. Chong TS, Tan ST, Fan WY (2006) *Chem A Eur J* 12:5128
177. Shi B, O'Brien RJ, Bao S, Davis BH (2001) *J Catal* 199:202
178. Taber DF, Kanai K, Jiang Q, Bui G (2000) *J Am Chem Soc* 122:6807

179. Glascoe EA, Sawyer KR, Shanoski JE, Harris CB (2007) *J Phys Chem C* 111:8789
180. Sawyer KR, Glascoe EA, Cahoon JF, Schlegel JP, Harris CB (2008) *Organometallics* 27:4370
181. Navarro RM, Pena MA, Fierro JLG (2007) *Chem Rev* 107:3952
182. Peters JW, Lanzilotta WN, Lemon BJ, Seefeldt LC (1998) *Science* 282:1853
183. Nicolet Y, de Lacey AL, Vernede X, Fernandez VM, Hatchikian EC, Fontecilla-Camps JC (2001) *J Am Chem Soc* 123:1596
184. Nicolet Y, Piras C, Legrand P, Hatchikian CE, Fontecilla-Camps JC (1999) *Structure* 7:13
185. Peters JW, Lanzilotta WN, Lemon BJ, Seefeldt LC (1998) *Science* 282:1853
186. Nicolet Y, de Lacey AL, Vernede X, Fernandez VM, Hatchikian EC, Fontecilla-Camps JC (2001) *J Am Chem Soc* 123:1596
187. Frey M (2002) *Chembiochem* 3:153
188. Volbeda A, Garcin E, Piras C, de Lacey AL, Fernandez VM, Hatchikian EC, Frey M, Fontecilla-Camps JC (1996) *J Am Chem Soc* 118:12989
189. Volbeda A, Charon M-H, Piras C, Hatchikian EC, Frey M, Fontecilla-Camps JC (1995) *Nature* 373:580
190. Volbeda A, Martin L, Cavazza C, Matho M, Faber BW, Roseboom W, Albracht SPJ, Garcin E, Rousset M, Fontecilla-Camps JC (2005) *J Biol Inorg Chem* 10:239
191. Ogata H, Hirota S, Nakahara A, Komori H, Shibata N, Kato T, Kano K, Higuchi Y (2005) *Structure* 13:1635
192. de Lacey AL, Fernandez VM, Rousset M (2005) *Coord Chem Rev* 249:1596
193. Vincent KA, Belsey NA, Lubitz W, Armstrong FA (2006) *J Am Chem Soc* 128:7448
194. Huhmann-Vincent J, Scott BL, Kubas GJ (1999) *Inorg Chim Acta* 294:240
195. Shima S, Pilak O, Vogt S, Schick M, Stagni MS, Meyer-Klaucke W, Warkentin E, Thauer RK, Ermler U (2008) *Science* 321:572
196. Gloaguen F, Lawrence JD, Rauchfuss TB (2001) *J Am Chem Soc* 123:9476
197. Gloaguen F, Lawrence JD, Rauchfuss TB, Bénard M, Rohmer M-M (2002) *Inorg Chem* 41:6573
198. Mejia-Rodriguez R, Chong D, Reibenspies JH, Soriaga MP, Darensbourg MY (2004) *J Am Chem Soc* 126:12004
199. Chong D, Georgakaki IP, Mejia-Rodriguez R, Sanabria-Chinchilla J, Soriaga MP, Darensbourg MY (2003) *Dalton Trans* 3:4158
200. Volkens PI, Rauchfuss TB (2007) *J Inorg Biochem* 101:1748
201. Felton GAN, Vannucci AK, Chen J, Lockett LT, Okumura N, Petro BJ, Zakai UI, Evans DH, Glass RS, Lichtenberger DL (2007) *J Am Chem Soc* 129:12521
202. Felton GAN, Vannucci AK, Okumura N, Lockett LT, Evans DH, Glass RS, Lichtenberger DL (2008) *Organometallics* 27:4671
203. Chiang M-H, Liu Y-C, Yang S-T, Lee G-H (2009) *Inorg Chem* 48:7604
204. Liu Z-P, Hu P (2002) *J Am Chem Soc* 124:5175
205. Fan H-J, Hall MB (2001) *J Am Chem Soc* 123:3828
206. Zampella G, Greco C, Fantucci P, De Gioia L (2006) *Inorg Chem* 45:4109
207. Greco C, Bruschi M, De Gioia L, Ryde U (2007) *Inorg Chem* 46:5911
208. Ohki Y, Yasumura K, Kuge K, Tanino S, Ando M, Li Z, Tatsumi K (2008) *Proc Natl Acad Sci USA* 105:7652
209. Li Z, Ohki Y, Tatsumi K (2005) *J Am Chem Soc* 127:8950
210. Tanino S, Li Z, Ohki Y, Tatsumi K (2009) *Inorg Chem* 48:2358
211. Perra A, Davies ES, Hyde JR, Wang Q, McMaster J, Schröder M (2006) *Chem Commun* 1103
212. Barton BE, Whaley CM, Rauchfuss TB, Gray DL (2009) *J Am Chem Soc* 131:6942
213. Yang X, Hall MB (2009) *J Am Chem Soc* 131:10901
214. Kirch M, Lehn J-M, Sauvage J-P (1979) *Helv Chim Acta* 62:1345
215. Moradpour A, Amouyal E, Keller P, Kagan H (1978) *Nouv J Chim* 2:547
216. Kalyanasundaram K, Kiwi J, Grätzel M (1978) *Helv Chim Acta* 61:2720

- 217. Krishnan CV, Sutin N (1981) *J Am Chem Soc* 103:2141
- 218. Goldsmith JJ, Hudson WR, Lowry MS, Anderson TH, Bernhard S (2005) *J Am Chem Soc* 127:7502
- 219. Tinker LL, McDaniel ND, Curtin PN, Smith CK, Ireland MJ, Bernhard S (2007) *Chem Eur J* 13:8726
- 220. Cline ED, Adamson SE, Bernhard S (2008) *Inorg Chem* 47:10378
- 221. Tinker LL, Bernhard S (2009) *Inorg Chem* 48:10507
- 222. Curtin PN, Tinker LL, Burgess CM, Cline ED, Bernhard S (2009) *Inorg Chem* 48:10498
- 223. Du P, Schneider J, Luo G, Brennessel WW, Eisenberg R (2009) *Inorg Chem* 48:4952
- 224. Du P, Knowles K, Eisenberg R (2008) *J Am Chem Soc* 130:12576
- 225. Zhang J, Du P, Schneider J, Jarosz P, Eisenberg R (2007) *J Am Chem Soc* 129:7726
- 226. Lazarides T, McCormick T, Du P, Luo G, Lindley B, Eisenberg R (2009) *J Am Chem Soc* 131:9192
- 227. Rau S, Schäfer B, Gleich D, Anders E, Rudolph M, Friedrich M, Görls H, Henry W, Vos JG (2006) *Angew Chem* 118:6361, *Angew Chem Int Ed* 45:6215
- 228. Elvington M, Brown J, Arachchige SM, Brewer KJ (2007) *J Am Chem Soc* 129:10644
- 229. Ozawa H, Haga M, Sakai K (2006) *J Am Chem Soc* 128:4926
- 230. Palmans R, Frank AJ (1991) *J Phys Chem* 95:9438
- 231. Na Y, Wang M, Pan J, Zhang P, Åkermark B, Sun L (2008) *Inorg Chem* 47:2805
- 232. Lomoth R, Ott S (2009) *Dalton Trans* 9952
- 233. Gärtner F, Sundararaju B, Surkus A-E, Boddien A, Loges B, Junge H, Dixneuf PH, Beller M (2009) *Angew Chem Int Ed* 48:9962
- 234. Kluwer AM, Kapre R, Hartl F, Lutz M, Spek AL, Brouwer AM, van Leeuwen PWNM, Reek JNH (2009) *Proc Natl Acad Sci* 106:10460
- 235. Knölker H-J, Goesmann H, Klauss R (1999) *Angew Chem Int Ed* 38:702
- 236. Mercury 2.2 for Windows. This material is available free of charge via the Internet at <http://www.ccdc.cam.ac.uk/mercury/>



<http://www.springer.com/978-3-642-14669-5>

Iron Catalysis  
Fundamentals and Applications  
Plietker, B. (Ed.)  
2011, XII, 220 p., Hardcover  
ISBN: 978-3-642-14669-5